

Linear-cost unbiased posterior estimates for crossed effects and matrix factorization models via couplings

Paolo Maria Ceriani^a and Giacomo Zanella^{a,b}

^a*Department of Decision Sciences, Bocconi University, Milan, Italy*

^b*Bocconi Institute for Data Science and Analytics, Bocconi University, Milan, Italy*

Abstract

We design and analyze unbiased Markov chain Monte Carlo (MCMC) schemes based on couplings of blocked Gibbs samplers (BGSs), whose total computational costs scale linearly with the number of parameters and data points. Our methodology is designed for and applicable to high-dimensional BGS with conditionally independent blocks, which are often encountered in Bayesian modeling. We provide bounds on the expected number of iterations needed for coalescence for Gaussian targets, which imply that practical two-step coupling strategies achieve coalescence times that match the relaxation times of the original BGS scheme up to a logarithmic factor. To illustrate the practical relevance of our methodology, we apply it to high-dimensional crossed random effect and probabilistic matrix factorization models, for which we develop a novel BGS scheme with improved convergence speed. Our methodology provides unbiased posterior estimates at linear cost (usually requiring only a few BGS iterations for problems with thousands of parameters), matching state-of-the-art procedures for both frequentist and Bayesian estimation of those models.

1 Introduction

In recent years, unbiased Markov Chain Monte Carlo via couplings (UMCMC) has emerged as a promising framework to remove bias from MCMC estimates, thus potentially allowing for early stopping, simplifying the convergence diagnostic process and facilitating parallelization (Glynn and Rhee, 2014; Jacob et al., 2020). In UMCMC, coupled chains are run for a random number of iterations (at least up to coalescence) and their values are combined to produce unbiased estimates. A natural question that arises is whether this class of estimates incurs a greater computational cost than conventional MCMC based on simple ergodic averages and to quantify this potential difference. Framing the question differently, one may ask whether it is possible to devise UMCMC methods with computational cost matching top performing MCMCs, while enjoying the above mentioned benefits.

On a different line of research, various works showed how carefully designed blocked Gibbs Samplers (BGSs), i.e. Gibbs sampling schemes that update entire blocks of coordinates jointly, can achieve state-of-the-art performances for sampling from the posterior distributions of various challenging high-dimensional Bayesian models, such as non-nested models with crossed dependencies (Papaspiliopoulos et al., 2019, 2023). In particular, BGSs achieve linear computational costs in the number of parameters and observations in asymptotic regimes where both diverge to infinity.

In this work, we seek to combine these two lines of research, aiming to design UMCMC BGS methods with linear computational cost in the aforementioned high-dimensional regimes. Specifically, we provide a theoretical contribution, i.e. the analysis of BGS couplings for Gaussian targets via explicit bounds on the expected number of iterations, showing that practical two-step BGS coupling schemes achieve coupling times that match relaxation times up to a logarithmic factor; and some methodological ones, discussing implementation aspects of couplings of BGS with conditionally independent blocks and developing a novel BGS scheme for probabilistic matrix factorization which empirically reduces the MCMC complexity to linear for those models. To illustrate the practical relevance of our methodology, we apply it to crossed random effect models (Gelman, 2005; Baayen et al., 2008), a commonly used class of additive models that connect a response variable to categorical predictors, and to probabilistic matrix factorization (PMF) models (Salakhutdinov and Mnih, 2008; Miller and Carter, 2020), which can be seen as dimensionality reduction models based on low-rank representations.

The remaining part of the article is organized as follows: after briefly presenting the objectives of the paper and the three running examples that motivate our research in Section 2, we review how to exploit couplings to obtain unbiased estimates in Section 3. The main theoretical results are presented in Section 4: we provide bounds on the expected number of iterations needed for coalescence of coupled chains and specialize it for different classes of Markov chains. We apply the methodology and the theoretical results to Gaussian crossed random effect models in Section 5, generalized linear mixed models (GLMMs) with crossed effects in Section 7 and to PMF models in Section 8. Section 6 discusses some methodological aspects related to couplings of BGS with conditionally independent blocks. The code to reproduce the simulations reported in this paper can be found at https://github.com/paoloceriani/couplings_bgs.

2 Motivation and objectives

Many high-dimensional Bayesian models with a high degree of conditional independence are well-suited for BGSs. For these classes of models, BGSs often achieve state-of-the-art performance and in particular, unlike most available sampling schemes, result in a total computational cost scaling linearly in the number of observations and parameters. In this paper we will consider the following three models as running examples motivating the methodology and theory developed later. Despite their relatively simple formulations, these models are computationally challenging to estimate: correlated errors lead to expensive GLS estimates and strong posterior dependence induced by observations results in slow mixing of standard MCMCs.

Model 1 (Gaussian crossed random effects). Cross-classified data, where each observation can be simultaneously classified according to two or more variables, are commonly found in the modern scientific literature, with applications in various domains including health and social sciences (Gelman, 2005; Baayen et al., 2008). More in detail, a univariate response variable y is assumed to depend additively on the unknown effects of K categorical variables, termed *factors*, each one with I_k different possible values, called *levels*, for $k = 1, \dots, K$. The effect of the i -th level of the k -th factor is described by a random variable $a_i^{(k)}$, object of inference. Let $\mathbf{a}^{(k)} = (a_1^{(k)}, \dots, a_{I_k}^{(k)})$ denote the I_k -dimensional vector of effects of the k -th factor, for $k = 1, \dots, K$; $\mathbf{y} = (y_n)_{n=1}^N$, $\mathbf{a} = (\mathbf{a}^{(k)})_{k=1}^K$ and $\boldsymbol{\tau} = (\tau_k)_{k=0}^K$ the vectors of all data, effects and precisions respectively. Furthermore let $i_k[n]$ denote the level of the k -th factor associated to the n -th observation (see e.g. Section 1.1 and Chapter 11 of Gelman and Hill (2006) for more details

on this notation). In this paper, for clarity of exposition, we will consider the intercept-only version, although the concepts discussed extend to more general versions with covariates as well as random slopes (Gao and Owen, 2016; Papaspiliopoulos et al., 2023). The model with its standard prior can then be written as

$$\begin{aligned}
y_n | \mu, \mathbf{a}, \tau_0 &\sim N\left(\mu + \sum_{k=1}^K a_{i_k[n]}^{(k)}, \tau_0^{-1}\right) & n = 1, \dots, N, \\
a_i^{(k)} | \tau_k &\sim N(0, \tau_k^{-1}) & i = 1, \dots, I_k, k = 1, \dots, K, \\
p(\tau_k) &\propto \tau_k^{-0.5} & \text{for } k = 0, \dots, K, \\
p(\mu) &\propto 1,
\end{aligned} \tag{1}$$

where μ is a random intercept. In (1), $p(\cdot)$ denotes the density of the random variable inside the brackets and $N(\mu, \sigma^2)$ denotes a Gaussian distribution with mean μ and variance σ^2 . We will often consider the model with $K = 2$ factors, where one can think of y_n as the rating that user $i_1[n]$ gave to film $i_2[n]$.

Model 2 (GLMMs with crossed effects). Generalized linear mixed models (GLMMs) extend the framework of linear mixed models to accommodate non-Gaussian response variables by incorporating a link function, but still retaining the same dependence structure. They are a powerful tool widely used in many academic fields, such as political science, biology and medicine; see e.g. (Wood, 2017, Ch.3) and Jiang and Nguyen (2021). Extending Model 1 to allow for general response gives

$$\mathcal{L}(y_n | \mu, \mathbf{a}) = \mathcal{L}(y_n | \eta_n) \text{ with } \eta_n = \mu + \sum_{k=1}^K a_{i_k[n]}^{(k)} \text{ for } n = 1, \dots, N, \tag{2}$$

where $\mathcal{L}(\cdot)$ denotes the law of the random variable within brackets. Different choices of the conditional distribution $\mathcal{L}(y_n | \eta_n)$ lead to different models, e.g. $\mathcal{L}(y_n | \eta_n) = N(\eta_n, \tau_0^{-1})$ is equivalent to Model 1 or $\mathcal{L}(y_n | \eta_n) = \text{Bern}(p)$ with $p = \frac{1}{1+e^{-\eta_n}}$ leads to a logit model for binary data. In Section 7 we will consider the case $\mathcal{L}(y_n | \mu, \mathbf{a}) = \text{Lapl}(\eta_n, 1/\sqrt{2})$, where $\text{Lapl}(\mu, b)$ denotes the univariate Laplace distribution with mean μ and scale b .

Model 3 (Probabilistic matrix factorization). Low rank matrix approximation methods provide one of the simplest and most effective approaches to collaborative filtering (Salakhutdinov and Mnih, 2008; Miller and Carter, 2020), i.e. forecasting of users' interests exploiting other users' preferences. As for Models 1 and 2 with $K = 2$, one can think of observation y_n as representing the rating that user $i[n]$ gives to film $j[n]$. Denoting by \mathbf{u}_i and \mathbf{v}_j respectively the d -dimensional latent user-specific and film-specific factors for $I = 1, \dots, I_1$ and $j = 1, \dots, I_2$, and by $\mathbf{u} = (\mathbf{u}_i)_{i=1}^{I_1} \in \mathbb{R}^{I_1 \times d}$, $\mathbf{v} = (\mathbf{v}_j)_{j=1}^{I_2} \in \mathbb{R}^{I_2 \times d}$ their collections, the model can be formulated as

$$\begin{aligned}
y_n | \rho, \mathbf{u}, \mathbf{v}, \tau_0 &\sim N(\rho \mathbf{u}_{i[n]}^\top \mathbf{v}_{j[n]}, \tau_0^{-1}) & n = 1, \dots, N, \\
\mathbf{u}_i, \mathbf{v}_j &\sim N(\mathbf{0}, 1_d) & i = 1, \dots, I_1, j = 1, \dots, I_2, \\
\tau_0 &\sim \text{Gamma}(c, d), & \rho^{-\frac{1}{2}} \sim \text{Gamma}(a, b),
\end{aligned} \tag{3}$$

where $\text{Gamma}(a, b)$ denotes a Gamma random variable with shape parameter a and scale parameter b , 1_d denotes the d -dimensional identity matrix and ρ indicates a positive quantity acting as scaling factor for the random effects. PMF models can be seen as a multiplicative extension

of the models in (1) and (2), and are usually more computationally challenging to estimate (due to invariances with respect to rotations, a lower degree of linearity, etc).

All the models above feature a small number of high-dimensional blocks whose conditional distributions are relatively easy to manage, while the joint distribution is computationally much harder to deal with. This is a common structure arising in Bayesian modelling scenarios (Gelman, 2005), and we expect the discussion below on couplings of BGS to be generally relevant to Bayesian models with sparse conditional independent structure where BGS perform well.

2.1 Asymptotic regimes of interest and computational cost

Models 1, 2 and 3 naturally lead to situations where both the number of observations N and parameters $p = O(\sum_{k=1}^K I_k)$ are large. We use the notation $(T_n)_{n \in \mathbb{N}} = O(f(n))$ if there exist constants $c, C \in \mathbb{R}$ with $0 < c < C < \infty$ such that $cf(n) \leq T_n \leq Cf(n)$ for all n . In the following we will talk about asymptotic regimes in terms of $N \rightarrow \infty$, implicitly assuming that p is a function of N that is also diverging as $N \rightarrow \infty$.

Also, the above models are commonly used in *sparse* settings, where a small fraction of the possible combinations of effects are observed, i.e. $N \ll \prod_{k=1}^K I_k$. For example, when $K = 2$ one often has $1 \ll p < N \ll I_1 \times I_2$ (see Gao and Owen (2016) for further discussion). Using the analogy of films and ratings for recommender systems, the above means assuming that the number of ratings, users and films is large, but only a small fraction of the film is rated by each user. Depending on the degree of sparsity in the observation design, one could have either $p = O(N)$ or $p/N \rightarrow 0$ as $N \rightarrow \infty$.

We consider the task of performing posterior inference for the above models using MCMC methods. We are interested in quantifying the computational effort needed for the posterior estimation (both in the MCMC and UMCMC context) as $N \rightarrow \infty$. In the (U)MCMC context, the total cost is defined as the product between the cost per iteration and the expected number of iterations for the convergence (coalescence) of the chains. As discussed below, recent works suggest that BGS can achieve state-of-the-art performances of $O(N)$ posterior estimation cost. Our main objective is to assess whether UMCMC methods with the same cost can be devised for this problem, as well as to provide some guidance on how to do so.

2.2 Related literature and block-updating schemes

Models with crossed dependencies are computationally harder than classical Bayesian hierarchical models with nested structures. For example, even in the Gaussian case (i.e. Model 1), evaluating the marginal likelihood once (e.g. computing $\mathcal{L}(\mathbf{y} \mid \boldsymbol{\tau}, \boldsymbol{\mu})$ for a given $\boldsymbol{\tau}$ and $\boldsymbol{\mu}$) requires the inversion of a $O(\sum_{k=1}^K I_k)$ -dimensional matrix. Despite the matrix being sparse, the crossed dependence structure leads to a dense Cholesky factor (Pandolfi et al., 2024, Sec.3), and more generally prevents the use of efficient sparse linear algebra tools available for, e.g., nested or spatial hierarchical model, leading to a computational cost of at least $O(N^{3/2})$ for each evaluation (Gao and Owen, 2016; Perry, 2017; Papaspiliopoulos et al., 2023; Menictas et al., 2023). The situation is obviously worse in the non-Gaussian case, where analogous computation involve general $O(\sum_{k=1}^K I_k)$ -dimensional integrals.

On the other hand, the above models lend themselves naturally to block updating schemes,

such as BGSs in the sampling context or block coordinate ascent (aka backfitting) for maximum a posteriori (MAP) or generalized least square (GLS) computations. For example, given the conditional independence structure of Model 1, the posterior conditional distribution of $\mathbf{a}^{(k)}$ factorizes as $\mathcal{L}(\mathbf{a}^{(k)}|\mu, \mathbf{a}^{(-k)}, \boldsymbol{\tau}, \mathbf{y}) = \otimes_{i=1}^{I_k} \mathcal{L}(a_i^{(k)}|\mu, \mathbf{a}^{(-k)}, \boldsymbol{\tau}, \mathbf{y})$, where \otimes denotes the product of independent distributions. Thus a BGS with components $\mu, \mathbf{a}^{(1)}, \dots, \mathbf{a}^{(K)}$ and $\boldsymbol{\tau}$, which we will call *vanilla* BGS, can be trivially implemented at $O(N)$ cost per iteration for Model 1. However, such vanilla version can mix slowly. In particular, Gao and Owen (2016) showed that for Model 1 with $K = 2$ factors, known variances and full observation designs, the vanilla BGS requires $O(\sqrt{N})$ to converge, leading to a prohibitive $O(N^{\frac{3}{2}})$ total cost. This follows from the fact that observed values create strong a posteriori dependence between unknown factors. Papaspiliopoulos et al. (2019) proposed a collapsed Gibbs Sampler (see Algorithm 2 below) which preserves the $O(N)$ cost per iteration and converges in $O(1)$ iterations under appropriate assumptions, see also (Papaspiliopoulos et al., 2023, Thm.2). Similar techniques have been employed to develop a *back-fitting* algorithm to perform GLS estimation for an analogue of Model 1 with $O(N)$ cost in Ghosh et al. (2022). A first question of interest that we consider is whether the same computational efficiency can be extended to the UMCMC context, which we answer positively in Section 5. The extension to the UMCMC case allows one to stop MCMC runs after few (e.g. around 10, see Section 5.3) iterations while still obtaining unbiased estimates, getting closer to what one could do in the GLS case (where backfitting is often reported to converge in few iteration, see e.g. the discussion in Ghosh et al. (2022, Section 7) about comparison between the cost of Bayesian and frequentist computations for those models).

3 Background on couplings for estimation and blocked Gibbs samplers

We now provide some background material on UMCMC and BGSs. Specifically, Section 3.2 provides a concise recap of how to exploit couplings for unbiased MCMC estimation, as presented in Jacob et al. (2020), while Sections 3.3 and 3.4 introduce, respectively, two-step coupling algorithms and BGS kernels.

3.1 Notation

In the following, vectors are denoted in bold, matrices in capital letters and univariate quantities in standard lowercase. We denote the space of probability measures over a space \mathcal{X} by $\mathcal{P}(\mathcal{X})$. Given $p, q \in \mathcal{P}(\mathcal{X})$, $\Gamma(p, q)$ is the set of couplings between p and q , i.e. joint distributions on $\mathcal{X} \times \mathcal{X}$ whose first and second marginals are, respectively, p and q . For a kernel P on \mathcal{X} , we denote by \bar{P} , or more explicitly $\bar{P}[P]$, a kernel on $\mathcal{X} \times \mathcal{X}$ such that $\bar{P}[P]((\mathbf{x}, \mathbf{y}), \cdot) \in \Gamma(P(\mathbf{x}, \cdot), P(\mathbf{y}, \cdot))$ for every $(\mathbf{x}, \mathbf{y}) \in \mathcal{X} \times \mathcal{X}$. We denote by $(p \otimes q) \in \mathcal{P}(\mathcal{X} \times \mathcal{Y})$ the product measure defined as $(p \otimes q)(A \times B) = p(A)q(B)$ for all $A \subseteq \mathcal{X}$ and $B \subseteq \mathcal{Y}$. With a slight abuse of notation we use $\Gamma(p, q)$ to denote both the collection of distributions and that of random variables, i.e. we also write $(\mathbf{X}, \mathbf{Y}) \in \Gamma(p, q)$ for random vectors (\mathbf{X}, \mathbf{Y}) such that $\mathbf{X} \sim p, \mathbf{Y} \sim q$. A coupling $(\mathbf{X}, \mathbf{Y}) \in \Gamma(p, q)$ is called *maximal* if it maximises the probability of equality between the two variables, i.e. if $\Pr(\mathbf{X} = \mathbf{Y}) = 1 - \|p - q\|_{TV}$ where $\|\cdot\|_{TV}$ denotes the norm induced by the total variation distance. We will denote by $\Gamma_{max}(p, q) \subset \Gamma(p, q)$ the collection of maximal couplings of p, q . Analogously, we write $\bar{P}[P] \in \Gamma_{max}[P]$ if $\bar{P}((\mathbf{x}, \mathbf{y}), \cdot) \in \Gamma_{max}(P(\mathbf{x}, \cdot), P(\mathbf{y}, \cdot))$ for every

$\mathbf{x}, \mathbf{y} \in \mathcal{X}$. For a recap on maximal couplings and algorithms, we refer to Section A.1 in the supplement.

A coupling $(\mathbf{X}, \mathbf{Y}) \in \Gamma(p, q)$ minimizing $\mathbb{E}[\|\mathbf{X} - \mathbf{Y}\|^2]$ among all couplings of p and q is called Wasserstein-2 (W_2) optimal, and we will denote the family of such optimal couplings as $\Gamma_{W_2}(p, q)$. Analogously, we say that \bar{P} is a W_2 -optimal coupling of a kernel P , and write $\bar{P}[P] \in \Gamma_{W_2}[P]$, if $\bar{P}[P](\mathbf{x}, \mathbf{y}, \cdot) \in \Gamma_{W_2}(P(\mathbf{x}, \cdot), P(\mathbf{y}, \cdot))$ for every $\mathbf{x}, \mathbf{y} \in \mathcal{X}$. See Section A.2 for basic notions of W_2 optimal couplings.

3.2 Background on UMCMC

We are interested in approximating expectations of the form

$$\mathbb{E}_\pi[h] = \int_{\mathcal{X}} h(\mathbf{x})\pi(d\mathbf{x}),$$

where $\pi \in \mathcal{P}(\mathcal{X})$ is the target probability and $h : \mathcal{X} \rightarrow \mathbb{R}$ a test function. Following Glynn and Rhee (2014) and Jacob et al. (2020), we consider unbiased estimators of $\mathbb{E}_\pi[h]$ based on coupled Markov chains that marginally evolve according to a common π -invariant transition kernel P .

Let $(\mathbf{X}^t, \mathbf{Y}^t)_{t \geq 0}$ be a Markov chain on $\mathcal{X} \times \mathcal{X}$ with coupled kernel $\bar{P}[P]$ such that: the two chains evolving according to \bar{P} must meet after finite time, i.e. if we define the meeting time $T = \min\{t \geq 0 : \mathbf{X}^t = \mathbf{Y}^t\}$, it must hold $\Pr(T < \infty) = 1$; and after meeting the two chains stay together, i.e. $\mathbf{X}^t = \mathbf{Y}^t$ for all $t \geq T$. The initial distribution is taken to be $(\mathbf{X}^0, \mathbf{Y}^0) \sim (\pi_0 P) \otimes \pi_0$ for some π_0 , meaning that we initialize $\mathbf{X}^{-1} \sim \pi_0$ and $\mathbf{Y}^0 \sim \pi_0$, with \mathbf{X}^{-1} and \mathbf{Y}^0 independent, and then take $\mathbf{X}^0 | \mathbf{X}^{-1} \sim P(\mathbf{X}^{-1}, \cdot)$.

Under the above assumptions and some regularity conditions on the distribution of T (see Sec.2.1 of Jacob et al. (2020) or milder conditions in Middleton et al. (2020)), the random variable

$$H_k((\mathbf{X}^t)_{t \geq 1}, (\mathbf{Y}^t)_{t \geq 1}) = h(\mathbf{X}^k) + \sum_{t=k+1}^{T-1} (h(\mathbf{X}^t) - h(\mathbf{Y}^t)) \quad k \geq 0,$$

is an unbiased estimator of $\mathbb{E}_\pi[h]$. Note that $H_k = h(\mathbf{X}^k)$ if $k+1 > T-1$. Taking the average of H_l for $l \in \{k, \dots, m\}$, where k is a burn-in value and m a maximum number of iterations, leads to the unbiased estimator

$$\begin{aligned} H_{k:m}((\mathbf{X}^t)_{t \geq 1}, (\mathbf{Y}^t)_{t \geq 1}) &= \frac{1}{m-k+1} \sum_{l=k}^m h(\mathbf{X}^l) \\ &+ \sum_{l=k+1}^{T-1} \min\left(1, \frac{l-k}{m-k+1}\right) (h(\mathbf{X}^l) - h(\mathbf{Y}^l)) \quad 0 \leq k < m, \end{aligned}$$

which coincides with the usual MCMC ergodic average estimate plus a bias correction term. Standard guidelines in Jacob et al. (2020) suggest to choose k as a large quantile of the meeting time T and m as a multiple of k . Hence, for the method to be most practical, the meeting time should occur as early as possible.

3.3 Two-step couplings

In this paper we consider kernels \bar{P} that follow a two-step strategy: whenever the chains are “far away” we employ a *contractive* coupling \bar{P}^c whose aim is to bring the chains closer to each other (see e.g. Section 6); when the chains are “close enough” we employ a maximal coupling \bar{P}^m (see e.g. Algorithm 5 or Algorithm 6 in the supplement), which maximizes the probability of the chains being exactly equal at the next step. The resulting kernel \bar{P} takes the form

$$\bar{P}[P]((\mathbf{x}, \mathbf{y}), \cdot) = \begin{cases} \bar{P}^c[P]((\mathbf{x}, \mathbf{y}), \cdot) & \text{if } d(\mathbf{x}, \mathbf{y}) > \varepsilon \\ \bar{P}^m[P]((\mathbf{x}, \mathbf{y}), \cdot) & \text{if } d(\mathbf{x}, \mathbf{y}) \leq \varepsilon, \end{cases} \quad (4)$$

where $d(\mathbf{x}, \mathbf{y})$ is a measure of distance between \mathbf{x} and \mathbf{y} , such as $d(\mathbf{x}, \mathbf{y}) = \|P(\mathbf{x}, \cdot) - P(\mathbf{y}, \cdot)\|_{TV}$ or $d(\mathbf{x}, \mathbf{y}) = \|\mathbf{x} - \mathbf{y}\|$, and ε is a threshold parameter. Algorithm 1 provides a pseudo-code implementing this strategy.

Algorithm 1: Two-step coupling algorithm

Input: initial distribution π_0 , kernels P , \bar{P}^c , \bar{P}^m

sample $\mathbf{X}^{-1} \sim \pi_0$, $\mathbf{Y}^0 \sim \pi_0$ and $\mathbf{X}^0 \sim P(\mathbf{X}^{-1}, \cdot)$ **while** $\mathbf{X}^t \neq \mathbf{Y}^t$ **do**

if $d(\mathbf{X}^t, \mathbf{Y}^t) > \varepsilon$ **then**
 | $(\mathbf{X}^{t+1}, \mathbf{Y}^{t+1}) \sim \bar{P}^c[P]((\mathbf{X}^t, \mathbf{Y}^t), \cdot)$
 else
 | $(\mathbf{X}^{t+1}, \mathbf{Y}^{t+1}) \sim \bar{P}^m[P]((\mathbf{X}^t, \mathbf{Y}^t), \cdot)$
 | $t \leftarrow t + 1$

Output: trajectory $(\mathbf{X}^t, \mathbf{Y}^t)_{t \in \{0, \dots, T\}}$

Two-step couplings have been previously used in the literature, see e.g. Roberts and Rosenthal (2002); Alexandros and Roberts (2005); Bou-Rabee et al. (2020a); Biswas et al. (2022). The motivation behind this construction is that *one-step* couplings, which aim for exact chain meeting at each step, are generally suboptimal in terms of meeting times (Griffeath, 1975). The intuitive reason is that high meeting probability and effective contraction are typically separate qualities in couplings: when a maximal coupling fails, preserving marginals might imply sampling distant points in \mathcal{X} , thus reducing meeting probability in subsequent steps. Algorithm 1 avoids the previous issue by using \bar{P}^c and \bar{P}^m in order to, respectively, achieve optimal contraction rates and maximal meeting probabilities. In Section 6 we show how to design \bar{P}^c and \bar{P}^m in the BGS context for distributions with high degree of independence.

3.4 Blocked Gibbs Sampler kernels

We now formally define BGS kernels. Let $\mathbf{x} = (\mathbf{x}_{(1)}, \dots, \mathbf{x}_{(K)}) \sim \pi$, with $\pi \in \mathcal{P}(\mathcal{X})$ and $\mathcal{X} = \mathcal{X}_1 \times \dots \times \mathcal{X}_K$ partitioned in K blocks of dimension I_k for $k = 1, \dots, K$, i.e. $\mathbf{x}_{(k)} \in \mathcal{X}_k \subseteq \mathbb{R}^{I_k}$. We indicate by $\mathbf{x}_{(-k)} = (\mathbf{x}_{(j)})_{j \neq k}$ the whole vector except the k -th block and by $\pi(\mathbf{x}_{(k)} | \mathbf{x}_{(-k)})$ the so-called full conditional distribution of the k -th block. Various BGS variants can be derived depending on the chosen updating order. For example, the (deterministic-scan) *forward* version of BGS iteratively samples from $\pi(\mathbf{x}_{(k)} | \mathbf{x}_{(-k)})$ for $k = 1, \dots, K$ at each iteration. The resulting

kernel, which we denote as $P^{(F)}$, can be written as the following composition of K kernels

$$P^{(F)} = P_K \cdots P_1, \quad (5)$$

$$P_k(\mathbf{x}, d\mathbf{x}') = \pi(d\mathbf{x}'_{(k)} | \mathbf{x}_{(-k)}) \delta_{\mathbf{x}_{(-k)}}(d\mathbf{x}'_{(-k)}) \quad k = 1, \dots, K, \quad \mathbf{x} \in \mathcal{X}. \quad (6)$$

Other natural updating orders include the backward order, as well as the forward-backward or random-scan versions.

4 Bounds for couplings of Gaussian Gibbs Samplers

In this section we provide bounds on the meeting times of BGS coupled via Algorithm 1 when the target distribution is Gaussian. As discussed later in Section 4.2, we seek to obtain UMC schemes whose coupling times T are of the same order of (or not much greater than) the relaxation times of the original kernel P .

Algorithmic specification 1. For all the theoretical results of this section, we consider Algorithm 1 with $\bar{P}^m[P]$ being the *maximal reflection coupling* reported in Algorithm 6 in the supplement, $\bar{P}^c[P]$ being the common random numbers (*crn*) coupling reported in Lemma 6 and (64) in the supplement, and $d(\mathbf{x}, \mathbf{y}) = \|P(\mathbf{x}, \cdot) - P(\mathbf{y}, \cdot)\|_{TV}$. We defer more discussion on general specifications and implementations of Algorithm 1 to Section 6.

Throughout this section we take $\mathcal{X}_k = \mathbb{R}^{I_k}$ for $k = 1, \dots, K$, so that $\mathcal{X} = \mathbb{R}^d$ with $d = I_1 + \dots + I_K$, and $\pi = N(\boldsymbol{\mu}, \Sigma)$ a d -dimensional multivariate Gaussian. In this case, the Markov chain induced by BGS takes the form of a Gaussian auto-regression. We formally state it as a lemma below, where we also provide an expression for the associated relaxation time, which will be useful later. Recall that the *relaxation time* of an irreducible π -reversible kernel P is defined as $T_{rel} := 1/AbsGap(P)$, where $AbsGap(P) = 1 - \sup_{\lambda \in \sigma(P), |\lambda| \neq 1} |\lambda|$ is the (absolute) spectral Gap of P and $\sigma(P)$ denotes the spectrum of P . Relaxation times are closely related to mixing times (see e.g. Levin and Peres (2017, Section 12)) and can be interpreted as the number of iterations needed for the chain to be ε close to the target distribution, up to a multiplicative factor that depends on ε and on the starting distribution (see also Rosenthal (2003) for more discussion on the link between convergence, asymptotic variances and the spectrum of reversible Markov chains).

Lemma 1. *Let $\pi = N(\boldsymbol{\mu}, \Sigma)$ and P be a BGS kernel with updating order given by $(k_1, \dots, k_s) \in \{1, \dots, K\}^s$ for some $s \in \mathbb{N}$, i.e. $P = P_{k_s} \cdots P_{k_1}$ with P_k defined in (6). Then, one has*

$$P(\mathbf{x}, \cdot) = N\left(B\mathbf{x} + \mathbf{b}, \Sigma - B\Sigma B^\top\right), \quad (7)$$

where B depends on the updating order (k_1, \dots, k_s) and on the target precision matrix $Q = \Sigma^{-1}$, and $\mathbf{b} = (I - B)\boldsymbol{\mu}$. Furthermore the relaxation time of P is given by $T_{rel} = 1/(1 - \rho(B))$, where $\rho(B)$ denotes the largest modulus eigenvalue of B .

Lemma 1 is a well-known result, whose proof we omit, see e.g. Roberts and Sahu (1997, Lemma 1) for the explicit expression of B in the forward updating case, corresponding to $s = K$, $k_i = i$ for all i and $P = P^{(F)}$.

4.1 Bound for reversible chains

Our first bound applies to π -reversible BGS kernels, i.e. one where the updating order satisfies $(k_1, \dots, k_s) = (k_s, \dots, k_1)$. A classical example is the forward-backward kernel, defined as

$$P^{(FB)} = P_1 \cdots P_{K-1} P_K P_{K-1} \cdots P_1. \quad (8)$$

Algorithmically, $P^{(FB)}$ performs updates from $\pi(\mathbf{x}_{(k)} \mid \mathbf{x}_{(-k)})$ sequentially for $k = 1, 2, \dots, K-1, K, K-1, \dots, 2, 1$. If P is a π -reversible BGS kernel, it holds $\Sigma B^\top = B \Sigma$, with B as in Lemma 1 (see e.g. Proposition 4.27 of Khare and Zhou (2009)). This allows for neater theoretical results. In Section 4.4 we extend the result to non-reversible Gibbs samplers, such as those generated by the forward kernel $P^{(F)}$ in (5), where the result requires additional technical assumptions.

Theorem 1 (Bound for reversible chains). *Let $\pi = N(\boldsymbol{\mu}, \Sigma)$ and $(\mathbf{X}^t, \mathbf{Y}^t)_{t \geq 0}$ be a Markov chain marginally evolving with π -invariant BGS kernel and coupled via Algorithm 1 with Algorithmic specification 1. Then $T := \min\{t \geq 0 : \mathbf{X}^t = \mathbf{Y}^t\}$ satisfies*

$$\mathbb{E}[T \mid \mathbf{X}^0, \mathbf{Y}^0] \leq 4 + \frac{1}{-\ln(\rho(B))} \left[-\frac{1}{2} \ln(1 - \lambda_{\min}(B)^2) + C_0 + C_\varepsilon \right], \quad (9)$$

where λ_{\min} denotes the minimum norm of the eigenvalues, B is as in (7), $C_0 := \ln(\|L^{-1}(\mathbf{X}^0 - \mathbf{Y}^0)\|)$ with L such that $LL^\top = \Sigma$, and $C_\varepsilon \leq 6 \operatorname{erf}^{-1}(\varepsilon) - \ln(\operatorname{erf}^{-1}(\varepsilon))$, for erf^{-1} the inverse error function and $\operatorname{erf}(x) = \frac{2}{\sqrt{\pi}} \int_0^x e^{-t^2} dt$.

Remark 1. Both the distribution of T and the bound in (9) are invariant under block diagonal linear transformations that preserve the K -partite block structure of $(\mathbf{x}_{(1)}, \dots, \mathbf{x}_{(K)})$. See Section D.1.3 in the Supplement for a more detailed statement and proof.

For the proof of Theorem 1 we exploited the following bound for the expected squared distance between Gaussian distributions coupled via reflection maximal coupling which can be of independent interest.

Lemma 2. *Let $p = N(\boldsymbol{\xi}, \Sigma)$ and $q = N(\boldsymbol{\nu}, \Sigma)$ be d -dimensional Gaussians, and $(\mathbf{X}, \mathbf{Y}) \in \Gamma_{\max}(p, q)$ coupled via maximal reflection coupling (see e.g. Algorithm 6). If $\|\Sigma^{-1/2}(\boldsymbol{\xi} - \boldsymbol{\nu})\|^2 \leq 1$, then for every $A \in \mathbb{R}^{d \times d}$ it holds*

$$\mathbb{E}[\|A(\mathbf{X} - \mathbf{Y})\|^2 \mid \mathbf{X} \neq \mathbf{Y}] \leq \frac{\|A(\boldsymbol{\xi} - \boldsymbol{\nu})\|^2}{\|\Sigma^{-1/2}(\boldsymbol{\xi} - \boldsymbol{\nu})\|^4} \left(12 + 8\sqrt{\frac{2}{\pi}} \right).$$

Note that, for fixed Σ and A , the bound in Lemma 2 scales as $O(\|\boldsymbol{\xi} - \boldsymbol{\nu}\|^{-2})$ as $\|\boldsymbol{\xi} - \boldsymbol{\nu}\| \rightarrow 0$, which can be easily checked to be the correct rate for $d = 1$.

4.2 Connection to relaxation times

Combining Theorem 1 with Lemma 1 leads to the following result.

Corollary 1. *Under the same assumptions of Theorem 1, we have*

$$\mathbb{E}[T \mid \mathbf{X}^0, \mathbf{Y}^0] \leq 4 + T_{\text{rel}} \left[\frac{1}{2} \ln(T_{\text{rel}}) + C_0 + C_\varepsilon \right], \quad (10)$$

where $T_{rel} := 1/(1 - \rho(B^{(FB)}))$.

Proof of Corollary 1. The result follows from (9), noting that $\frac{1}{-\ln(x)} < \frac{1}{1-x}$, $-\ln(1 - x^2) < \ln(1/(1 - x))$ for $x \in (0, 1)$ and the latter is monotonically increasing in x , hence allowing to substitute $\lambda_{min}(B^{(FB)})$ with the quantity $\rho(B^{(FB)})$, greater by definition. Then since $T_{rel} = 1/(1 - \rho(B^{(FB)}))$ by Lemma 1 we get the result. \square

Corollary 1 provides interesting insights and implications. In particular, interpreting T_{rel} as the number of iterations required for \mathbf{X}^t to converge, it suggests that in this context UMCMC provides unbiased estimates with an average number of iterations (and an overall computational cost) that is comparable to the minimal number of iterations required by standard MCMC to converge (up to a logarithmic factor). Also, from a high-dimensional asymptotics perspective, it also implies that whenever the relaxation time of BGS is bounded as the number of data point and parameter grows (see e.g. Section 5.2), then also the meeting time is bounded in expectation, meaning that UMCMC does not increase the overall complexity (while allowing for e.g. early stopping and parallelization). On the other hand, (10) implies that whenever the meeting times of the *two-step* strategy diverges for a chosen BGS scheme, also the respective T_{rel} diverges.

One could interpret Corollary 1 as a best-case result for UMCMC. The underlying assumption would be that obtaining coupling times that are of smaller order than T_{rel} is typically unfeasible. While we are not aware of rigorous results in this direction (i.e. showing that $\mathbb{E}[T]$ cannot be much smaller T_{rel} under appropriate conditions), this seems reasonable to assume given that, for example, T_{rel} provides lower bounds on total variation mixing times (Levin and Peres, 2017, Section 12) and that the quantiles of T can be used to derive non-asymptotic upper bounds on those (see e.g. equation (4) in (Biswas et al., 2019)). While interesting, we leave a more detailed and rigorous exploration of lower bounds to $\mathbb{E}[T]$ to future works.

4.3 Bound for two-block Gibbs samplers

We now consider the two-block case. In this context, it is possible to find a block-diagonal transformation, in the spirit of Remark 1, which allows for a direct extension of the bound in Theorem 1 also to the non-reversible kernel $P^{(F)}$.

Theorem 2. *Let $\pi = N(\boldsymbol{\mu}, \Sigma)$, $K = 2$ and $(\mathbf{X}^t, \mathbf{Y}^t)_{t \geq 0}$ be a Markov chain marginally evolving with $P^{(F)}$, coupled via Algorithm 1 with Algorithmic specification 1. Then*

$$\mathbb{E}[T | \mathbf{X}^0, \mathbf{Y}^0] \leq 5 + T_{rel} [C_0 + C_\varepsilon], \quad (11)$$

where $T_{rel} = 1/(1 - \rho(B^{(F)}))$, $B^{(F)}$ as in (7), and (T, C_0, C_ε) as in Theorem 1.

Note that in contrast to Corollary 1, the bound has the same order of magnitude of T_{rel} without additional logarithmic terms.

4.4 Bound non-reversible case Gibbs samplers

We have the following result for the case of BGS with general updating order.

Theorem 3. Let $\pi = N(\boldsymbol{\mu}, \Sigma)$ and $(\mathbf{X}^t, \mathbf{Y}^t)_{t \geq 0}$ be a Markov chain evolving with kernel P as in (7), coupled via Algorithm 1, with Algorithmic specification 1. For any $\delta > 0$, it holds that

$$\mathbb{E}[T | \mathbf{X}^0, \mathbf{Y}^0] \leq 4 + 3 \max \left(n_\delta^*, (1 + \delta) T_{rel} \left[-\frac{1}{2} \ln(1 - \lambda_{\min}(NN^\top)) + C_0 + C_\varepsilon \right] \right), \quad (12)$$

with $T_{rel} = 1/(1 - \rho(B))$, $N = L^{-1}BL$, $(T, C_0, C_\varepsilon, L)$ as in Theorem 1, and

$$n_\delta^* := \inf \left\{ n_0 \geq 1 : \forall n \geq n_0 \quad 1 - \|N^n\|_2^{\frac{1}{n}} \geq \frac{1 - \rho(N)}{1 + \delta} \right\}.$$

The bound in (12) features the additional term n_δ^* . The reason for it is that, due to the non-reversibility of P , N is generally not symmetric. Thus $\|N^n\|_2^{\frac{1}{n}} \rightarrow \rho(N)$ from above (Gelfand, 1941), but in general $\|N^n\|_2^{\frac{1}{n}} \neq \rho(N)$ for finite n . In order to make the result in (12) fully informative, like the ones in the reversible and two-block cases, one would need to provide an explicit bound on n_δ^* for the given matrix N under consideration. In all our numerical experiments we observed n_δ^* to be smaller than the second term and never the leading term of the bound, and we expect it to be well-behaved in our contexts of interest. On the other hand, we are not aware of general tight bounds for n_δ^* and we thus left it as an explicit term in the bound.

Remark 2. Since the focus of this section is primarily to provide explicit and sharp bounds on $\mathbb{E}[T]$ for Gaussian BGS schemes, we did not specifically address issues related to the regularity assumptions necessary for the validity and finite variance of the unbiased estimator. However, we expect that the proofs of this section can be extended quite naturally to control higher moments of T , e.g. proving $\mathbb{E}[T^k] < +\infty$ for $k > 1$. In view of Theorem 2.1 in Atchadé and Jacob (2024), this would imply finite variance of the unbiased estimator.

5 Application to Gaussian crossed random effect models

In this section we combine the findings of Section 4 with existing results on Model 1. We highlight that all the theoretical results we will derive hold under the assumption of fixed $\boldsymbol{\tau}$ in (1) of Model 1. We first describe in Section 5.1 state-of-the-art marginal algorithms for Model 1, then present in Section 5.2 the resulting bound for meeting times if a two-step coupling is implemented and finally report numerical simulations in Section 5.3.

5.1 Collapsed Gibbs sampler for Model 1

Despite the favourable cost per iteration of the vanilla Gibbs sampler for Model 1 presented in Section 2.2, there are many settings of interest where its mixing is provably poor, often leading to a super linear overall computational cost. Paspaliopoulos et al. (2019) noted that integrating out the global mean μ while updating the remaining regression parameters in K blocks, leads to a much more efficient (i.e faster mixing) updating scheme, while preserving the same $O(N)$ cost per iteration of vanilla BGS. The resulting algorithm is called *collapsed Gibbs sampler* (Paspaliopoulos et al., 2019) and reported in Algorithm 2: at every iteration we first sample from $\mathcal{L}(\mu | \mathbf{a}^{(-k)}, \boldsymbol{\tau}, \mathbf{y})$ and then iteratively update the factor effect block from $\mathcal{L}(\mathbf{a}^{(k)} | \mu, \mathbf{a}^{(-k)}, \boldsymbol{\tau}, \mathbf{y})$, repeating the procedure for $k = 1, \dots, K$. The exact form of the full conditionals is reported in

Section C.1 of the supplement.

Algorithm 2: One iteration of the collapsed Gibbs sampler for Model 1

```

for  $k=1, \dots, K$  do
  draw  $\mu \sim \mathcal{L}(\mu | \mathbf{a}_{(-k)}, \boldsymbol{\tau}, \mathbf{y})$ 
  for  $i=1, \dots, I_k$  do
    draw  $a_i^{(k)} \sim \mathcal{L}(a_i^{(k)} | \mathbf{a}_{(-k)}, \mu, \boldsymbol{\tau}, \mathbf{y})$ 
  draw  $\tau_k \sim \mathcal{L}(\tau_k | \mathbf{a}, \mu, \boldsymbol{\tau}_{-k}, \mathbf{y})$ 
draw  $\tau_0 \sim \mathcal{L}(\tau_0 | \mathbf{a}, \mu, \boldsymbol{\tau}_{-0}, \mathbf{y})$ 

```

5.2 Bound on meeting times under random design assumptions

For Model 1 with $K = 2$ factors, balanced level designs (i.e. the same number of observations is observed for every level of each factor) and fixed $\boldsymbol{\tau}$, Papaspiliopoulos et al. (2019) show that the relaxation time of the collapsed algorithm, denoted by T_{cg} , is upper bounded by $T_{cg} \leq C T_{aux}$, where $C = 1 + \frac{\tau_0}{\min\{\tau_1, \tau_2\}}$ is constant with respect to N and p , and T_{aux} is the relaxation time of the auxiliary two-block Gibbs sampler on the discrete space $\{1, \dots, I_1\} \times \{1, \dots, I_2\}$ with invariant distribution $\Pr((i, j)) = n_{ij}/N$, where $n_{ij} = \sum_{n=1}^N \mathbb{I}(i_1[n] = i) \mathbb{I}(i_2[n] = j)$ denotes the number of observations of level i of factor 1 and j of factor 2. Under random design assumptions, the quantity T_{aux} can be bounded using random graph theory results, as done in Papaspiliopoulos et al. (2023). In particular, for N multiple of d_1 and d_2 , denote by $\mathcal{D}(N, d_1, d_2)$ the collection of all the possible observation patterns with exactly N observations, $I_1 = N/d_1$, $I_2 = N/d_2$ and binary balanced levels (i.e. there must be exactly d_1 and d_2 observations for each level of factor 1 and 2 respectively and $n_{ij} \in \{0, 1\}$ for all $i = 1, \dots, I_1$ and $j = 1, \dots, I_2$). Then, supposing uniformly at random designs among $\mathcal{D}(n, d_1, d_2)$ with $d_1, d_2 > 4$, one has

$$T_{aux} \leq 1 + \frac{2}{\sqrt{\min\{d_1, d_2\} - 2}} + \gamma,$$

asymptotically almost surely as $N \rightarrow +\infty$, for every $\gamma > 0$. The result follows from relating T_{aux} to the spectrum of a random bipartite bi-regular graph, and then applying an extension of the Friedman's second largest eigenvalue theorem to bipartite graphs developed in Brito et al. (2018). Combining the above with Theorem 2, we obtain the following bound for the expected meeting times.

Corollary 2. *Let $(\mathbf{X}^t, \mathbf{Y}^t)_{t \geq 0}$ be as in Theorem 2, where P is the collapsed Gibbs kernel (Algorithm 2) and let $\pi = N(\boldsymbol{\mu}, \boldsymbol{\Sigma})$ be the posterior distribution of Model 1 with $K = 2$ factors, fixed $\boldsymbol{\tau}$ and design $(n_{ij})_{i,j}$ picked uniformly at random from $\mathcal{D}(n, d_1, d_2)$. Then*

$$\Pr \left(\mathbb{E}[T | \mathbf{X}^0, \mathbf{Y}^0] \leq 5 + \left(1 + \frac{\tau_0}{\min\{\tau_1, \tau_2\}} \right) \left(1 + \frac{2}{\sqrt{\min\{d_1, d_2\} - 2}} + \gamma \right) [C_0 + C_\varepsilon] \right) \rightarrow 1,$$

as $N \rightarrow +\infty$, with (T, C_ε, C_0) as in Theorem 2, and the probability is with respect to the randomness of the design.

Interestingly, Corollary 2 provides an upper bound on the average coupling time that remains bounded as N (and p) diverge. In the next section we explore numerically the tightness of the

bound, and its robustness to the specific assumptions used to derive it.

5.3 Numerics

We compare the bounds of Theorems 1, 2 and 3 with the average meeting times of simulated coupled chains for both the vanilla and collapsed Gibbs samplers of Sections 2.2 and 5.1, for synthetic and real data in Section 5.3.1 and 5.3.3 respectively. Although the bounds are valid only for Gaussian chains (hence for Model 1 with fixed τ), we compare them with the average meeting times of coupled chains with known (i.e. fixed) as well as unknown (i.e. assigning to it a prior and including it into the Bayesian model) τ , yielding similar behaviours. The results support the intuition that, for the models under consideration, the convergence properties of the known and unknown variances case are very similar and thus the bounds are reasonably predictive also of the behaviour in the practically-used unknown variance case.

Algorithmic specification 2. We implement the two-step coupling procedure of Algorithm 1 for both the vanilla and the collapsed Gibbs sampler of Algorithm 2, with the standard priors in (1). More precisely, we use the block-wise coupling reported (13) and (14) (see Section 6 for further details), with maximal reflection coupling of Algorithm 6 as $\bar{P}_{max}[P_k]$ whenever implementable (e.g. Gaussian with same variance), or Algorithm 5 otherwise; $\bar{P}_{W_2}[P_k]$ is the *crn* coupling of Lemma 6. The distance in Algorithm 1 is set to $d(\mathbf{X}^t, \mathbf{Y}^t) = \|\mathbf{X}^t - \mathbf{Y}^t\|$ and the threshold parameter $\varepsilon = O((KI)^{-1})$.

Remark 3. The bounds of Theorems 1, 2, 3 are derived for strategies implementing $\bar{P}_{max}[P]$ and $\bar{P}_{W_2}[P]$, respectively maximal reflection and W_2 optimal couplings of the kernel P in (7). For ease of implementation, in this section we run simulations with successive composition of $\bar{P}_{max}[P_k]$ and $\bar{P}_{W_2}[P_k]$ for $k = 1, \dots, K$ as in (13) and (14), hence obtaining in principle worse performing couplings. We highlight that for Gaussian distributions (14) is actually equivalent to the W_2 optimal and $\bar{P}_{max}[P]$ is implementable with a computational cost of the same order of (13). A detailed proof of the equivalence of the costs is deferred to Section D.4 of the supplement.

5.3.1 Simulated data

We simulate data according to Model 1, with $\tau_0 = \tau_1 = \dots = \tau_k = 1$, $I_1 = \dots = I_K = I$ for fixed I , and different number of factors K . Observations are generated according to two different asymptotic regimes, with completely missing at random designs.

Asymptotic regime 1. Each combination of factor levels is either observed once or not with probability $p = 0.1$ independently from the rest, i.e. $n_{ij}^{(s,l)} \stackrel{iid}{\sim} \text{Bern}(p)$ for $i = 1, \dots, I_s$, $j = 1, \dots, I_l$ and $s \neq l \in \{1, \dots, K\}$, where $n_{ij}^{(s,l)} = \sum_{n=1}^N \mathbb{I}(i_s[n] = i) \mathbb{I}(i_l[n] = j)$ denotes the number of observations of level i of factor s and j of factor l . In this regime, one has $I = O(N^{1/K})$.

Asymptotic regime 2. Same as Regime 1 but with $p = 10/I^{K-1}$. This regime induces more sparsity, e.g. one has $I = O(N)$.

We plot the average of the meeting times as a function of the total number of parameters of the model, i.e. $1 + KI$ plus the number of scale parameters if any. Figure 1 reports results for the collapsed Gibbs sampler coupled with Algorithmic specification 2, for $K = 2$, $I_1 = I_2 = I \in \{50, 100, 250, 500, 1000\}$ levels, fixed and free variances. The bound of Theorem 2 for the two

blocks collapsed Gibbs sampler with fixed variances (using the true generating values) is also reported. The left and right panel corresponds, respectively, to Regime 1 and Regime 2. The

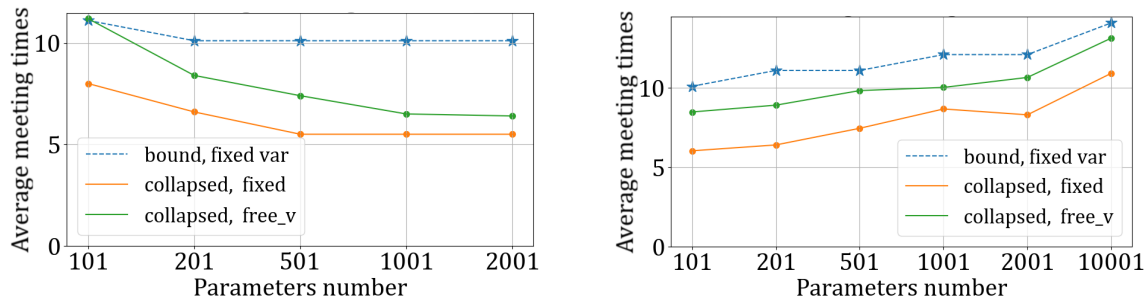


Figure 1: Estimated meeting times and bounds for $K = 2$, $I_1 = I_2 = I \in \{50, 100, 250, 500, 1000\}$, $\tau_0 = \tau_1 = \tau_2 = 1$ for Algorithm 2. Left: Regime 1, right: Regime 2.

results yield remarkably low meeting times and highlight a close resemblance of the meeting time behaviour with that of the bound. As a comparison, we report in Figure 2 the results for the vanilla algorithm on the same model. As expected, the provably higher relaxation time of

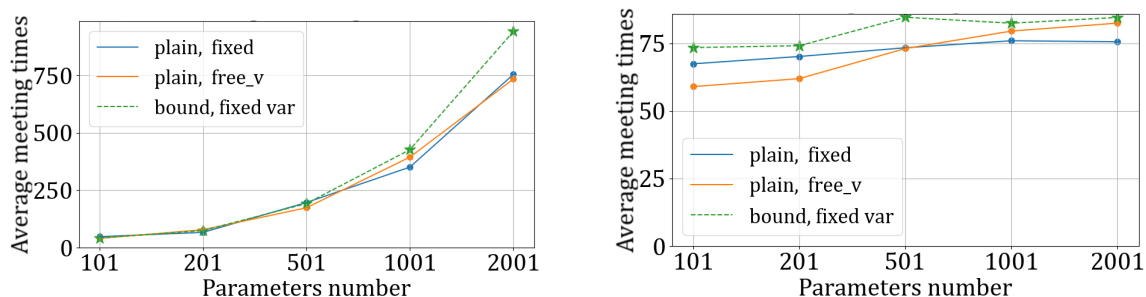


Figure 2: Estimated meeting times and bounds for $K = 2$, $I_1 = I_2 = I \in \{50, 100, 250, 500, 1000\}$, $\tau_0 = \tau_1 = \tau_2 = 1$, for plain vanilla algorithm. Left: Regime 1, right: Regime 2.

the vanilla Gibbs scheme results in an higher bound and, more importantly, higher on average meeting times of the coupled chains.

In Figure 3 we report the average meeting times for $K = 3$ (left) and $K = 4$ (right) factors, only for Regime 2, and the bound of Theorem 3. For these models the relaxation time is not computable explicitly even under the usual simplifying assumptions (fixed variances and balanced levels or cells), see e.g. Papaspiliopoulos et al. (2019). Thus proving scalability of the meeting times (or lack thereof), in light of Theorem 3, provide interesting insights on the mixing properties of the single chains themselves.

5.3.2 One-step vs two-step couplings

In Figure 4 we report the estimated distribution of meeting times for the collapsed Gibbs scheme with Algorithmic specification 2, when traditional or *two-step* coupling is implemented on a synthetic dataset with $K = 3$ factors and Regime 2. As can be seen from the above, the distribution of meeting times for the *two-step* strategy is more concentrated on smaller values

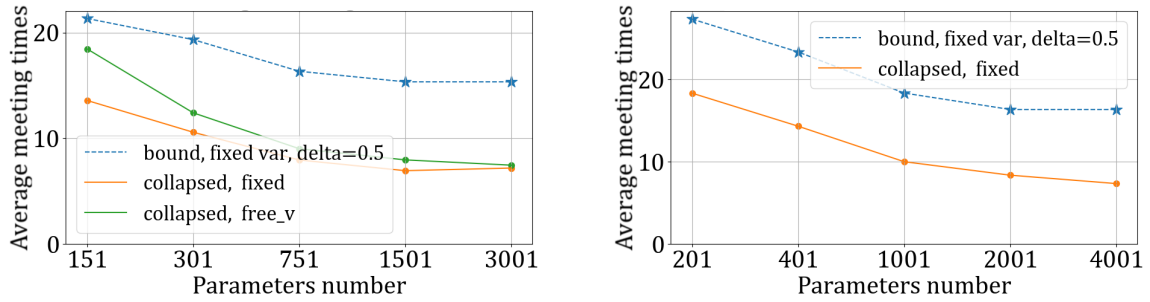


Figure 3: Estimated mean number of iterations and bounds for $K = 3$ (left), $K = 4$ (right), $I_1 = \dots = I_4 = I \in \{50, 100, 250, 500, 1000\}$, $\tau_k = 1$ for $k \in \{0, 1, 2, 3, 4\}$. Regime 2, Algorithm 2.

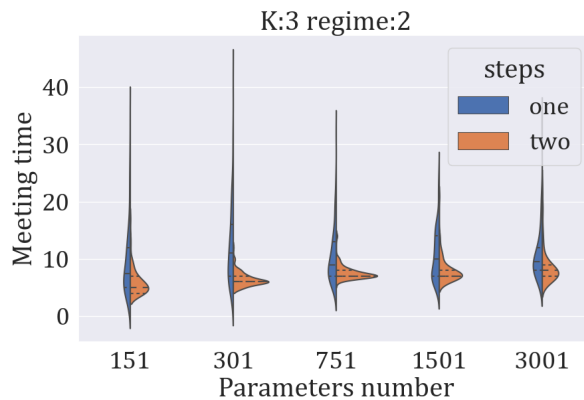


Figure 4: Estimated distribution of meeting times for $K = 3$, $I_1 = \dots = I_3 = I \in \{50, 100, 250, 500, 1000\}$, $\tau_k = 1$ for $k \in \{0, 1, 2, 3\}$ one vs two-step. Regime 2, Algorithm 2.

with considerably lighter tails, thus supporting the choice of a two-step coupling. On the other hand, we see that, in our context, using one- versus two- step coupling is less influential than, for example, in the one of (Biswas et al., 2022, Fig.3).

5.3.3 Real data example

We now consider a real dataset, containing university lecture evaluations by students at ETH Zurich. The dataset is freely available from the R package **lme4** (Bates et al., 2015) under the name “InstEval”. Each observation includes a score ranging from 1 to 5, assigned to a lecture, along with 6 factors that may potentially impact the score, including the identity of the student giving the rating or department that offers the course. Following the notation in (1), we have $N = 73421$, $K = 6$ and $(I_1, \dots, I_6) = (2972, 1128, 4, 6, 2, 14)$. We implement the two-step coupling with Algorithmic specification 2. We compute the estimated meeting times for different numbers and combinations of factors for Model 1 with fixed variances (estimated via standard MCMC and plugged in the coupling procedure). We numerically computed the bound for each combination using the MCMC variance estimates. The results of the experiment are shown in Table 1.

Algorithm	Factor number	mean #iter	bound for fixed τ
collapsed	[1,2]	10.1	15
collapsed	[1,6]	9.3	17
vanilla	[1,2]	50.7	73
vanilla	[1,6]	127.6	69

Table 1: Average meeting times for InstEval Dataset

The fact that for the vanilla scheme the bound is smaller than the estimated meeting time is not undermining the validity of our theory: as highlighted in Remark 3 of Section 3, the bound is derived for strategies coupling directly the kernel P of (7), while for ease of implementation we used (13) and (14). Furthermore, the bound holds for $d(\mathbf{x}, \mathbf{y}) = \|P(\mathbf{x}, \cdot) - P(\mathbf{y}, \cdot)\|_{TV}$ while we used $d(\mathbf{x}, \mathbf{y}) = \|\mathbf{x} - \mathbf{y}\|$.

6 Coupling strategies for blocked Gibbs samplers

The current section discusses alternative coupling strategies for BGSs with high degrees of conditional independence, providing some justification to the ones employed in Sections 4 and 5.3. Specifically, Section 6.1 focuses on aspects related to the general structure of Gibbs samplers, namely the necessity to couple successively composed kernels, while Section 6.2 focuses on those related to the updates of conditionally independent blocks.

6.1 BGS and compositions of couplings

In order to implement Algorithm 1, we need to specify $\bar{P}^c[P]$ and $\bar{P}^m[P]$, where P is a BGS kernel. Since P is defined as a composition of kernels, i.e. $P = P_{k_s} \cdots P_{k_1}$ with $s \in \mathbb{N}$ and $(k_1, \dots, k_s) \in \{1, \dots, K\}^s$ as in Lemma 1, a natural strategy is to sequentially compose maximal or optimally contractive couplings of P_{k_i} for $i = 1, \dots, s$. We denote the resulting coupling kernels as

$$\bar{P}^{m*}((\mathbf{x}, \mathbf{y}), \cdot) := \bar{P}_{max}[P_{k_s}] \cdots \bar{P}_{max}[P_{k_1}]((\mathbf{x}, \mathbf{y}), \cdot) \quad \forall \mathbf{x}, \mathbf{y} \in \mathcal{X}, \quad (13)$$

$$\bar{P}^{c*}((\mathbf{x}, \mathbf{y}), \cdot) := \bar{P}_{W_2}[P_{k_s}] \cdots \bar{P}_{W_2}[P_{k_1}]((\mathbf{x}, \mathbf{y}), \cdot) \quad \forall \mathbf{x}, \mathbf{y} \in \mathcal{X}, \quad (14)$$

where $\bar{P}_{max}[P_k] \in \Gamma_{max}[P_k]$ and $\bar{P}_{W_2}[P_k] \in \Gamma_{W_2}[P_k]$ for all $k = 1, \dots, K$. By construction, both $\bar{P}^{m*}((\mathbf{x}, \mathbf{y}), \cdot)$ and $\bar{P}^{c*}((\mathbf{x}, \mathbf{y}), \cdot)$ belong to $\Gamma[P]$. In all implementations of Algorithm 1, we employ $\bar{P}^m[P] = \bar{P}^{m*}$ and $\bar{P}^c[P] = \bar{P}^{c*}$. The appeal of \bar{P}^{m*} and \bar{P}^{c*} is that, in order to implement them, one needs to work only with the individual full conditionals involved in the original BGS scheme, which are often available in closed form, while the joint distribution $P(\mathbf{x}, \cdot)$ might be harder to work with. Note that these strategies are not guaranteed to be optimal since in general one has $\bar{P}^{m*} \notin \Gamma_{max}[P]$ and $\bar{P}^{c*} \notin \Gamma_{W_2}[P]$. For example, in the case $P = P^{(F)}$, \bar{P}^{c*} coincides with the so-called Knothe-Rosenblatt map (Rosenblatt, 1952; Knothe, 1957) of $P^{(F)}(\mathbf{x}, \cdot)$ and $P^{(F)}(\mathbf{y}, \cdot)$, which is in general different from the optimal transport one (Santambrogio, 2015, Section 2.3). Nonetheless, we still observe very fast contraction of \bar{P}^{c*} in our numerics, which might be partly explained by the fact that in the Gaussian case one indeed has $\bar{P}^{c*} \in \Gamma_{W_2}[P]$, as shown below.

Lemma 3 (Optimality of composition of W_2 couplings for Gaussians). *Let $\pi = N(\boldsymbol{\mu}, \Sigma)$ and \bar{P}^{c*} as in (14), with $s = K$ and (k_1, \dots, k_K) being a permutation of $(1, \dots, K)$. Then for all integers $n \geq 1$ it holds $(\bar{P}^{c*})^n \in \Gamma_{W_2}[P^n]$.*

The proof of Lemma 3 builds upon well known results about contractive couplings of Gaussian distributions. Firstly we exploit the fact that the optimal transport map between Gaussian distributions whose variance covariance matrices commute is the *crn* coupling (see Lemma 6 in Section A.2 and Dowson and Landau (1982); Olkin and Pukelsheim (1982)). Then, given the autoregressive form of Gaussian Gibbs samplers of Lemma 1, it is possible to write explicitly the W_2 optimal coupling for such kernel (see (64) in the supplement). Lastly, it is left to prove that such coupling is indeed equivalent to \bar{P}^{c*} .

6.2 Couplings of conditionally independent blocks

We now discuss how to implement $\bar{P}_{max}[P_k]$ and $\bar{P}_{W_2}[P_k]$ in cases where the associated full conditional factorizes as

$$\pi(\mathbf{x}_{(k)} | \mathbf{x}_{(-k)}) = \otimes_{i=1}^{I_k} \pi(x_{(k),i} | \mathbf{x}_{(-k)}), \quad (15)$$

for $x_{(k),i}$ denoting the i -th component of the vector $\mathbf{x}_{(k)}$, i.e. $\mathbf{x}_{(k)} = (x_{(k),1}, \dots, x_{(k),I_k})$, and I_k is large.

By (15), independently sampling from the univariate distributions $\pi(x_{(k),i} | \mathbf{x}_{(-k)})$ is equivalent to sampling directly from the entire block $\pi(\mathbf{x}_{(k)} | \mathbf{x}_{(-k)})$. The same intuition extends to W_2 optimal couplings but not to maximal ones. In particular, one has that the product of independent W_2 -optimal couplings of $\pi(x_{(k),i} | \mathbf{x}_{(-k)})$ for $i = 1, \dots, I_k$ is W_2 -optimal for $\pi(\mathbf{x}_{(k)} | \mathbf{x}_{(-k)})$ while the same is not true for maximal ones. In particular, when p and q are two product measures, one has the following well-known facts, which we collect in a lemma whose proof we omit for brevity.

Lemma 4. *Let $p, q \in \mathcal{P}(\mathcal{X}_1 \times \dots \times \mathcal{X}_d)$ with $p = \otimes_{i=1}^d p_i$ and $q = \otimes_{i=1}^d q_i$. Then $\mu_i \in \Gamma_{W_2}(p_i, q_i)$ for all $i = 1, \dots, d$ implies $(\otimes_{i=1}^d \mu_i) \in \Gamma_{W_2}(p, q)$. On the contrary, $\mu_i \in \Gamma_{max}(p_i, q_i)$ for all $i = 1, \dots, d$ does not imply $(\otimes_{i=1}^d \mu_i) \in \Gamma_{max}(p, q)$ in general. In particular, one has*

$$\min_{i=1, \dots, d} \Pr_{max}(p_i, q_i) \geq \Pr_{max}(p, q) \geq \prod_{i=1}^d \Pr_{max}(p_i, q_i), \quad (16)$$

where we use the notation $\Pr_{max}(p, q) := 1 - \|p - q\|_{TV}$, and all the inequalities can be strict.

Lemma 4 implies that, under (15), we can simply take a contractive coupling $\bar{P}_{W_2}[P_k]$ which factorizes across coordinates. On the contrary, joint maximal couplings of $\pi(\mathbf{x}_{(k)} | \mathbf{x}_{(-k)})$ do not factorize across coordinates under (15). The lower bound $\Pr_{max}(p, q) \geq \prod_{i=1}^d \Pr_{max}(p_i, q_i)$ in (16) implies that setting $\|p_i, q_i\|_{TV} = O(d^{-1})$ ensures $\Pr_{max}(p, q)$ is bounded away from 0. Lemma 5 quantifies the tightness of such lower bound for d -dimensional Gaussian distributions with same variance covariance matrix. We consider the regime where d goes to infinity and the distance between each rescaled mean decreases with d , which is arguably descriptive of what happens when using the two-step algorithm (Algorithm 1) of Section 3.3 in high dimensions.

Lemma 5. Consider $p = N(\boldsymbol{\mu}, \text{diag}(\boldsymbol{\sigma}))$ and $q = N(\boldsymbol{\nu}, \text{diag}(\boldsymbol{\sigma}))$, d -dimensional Gaussian distribution with $\boldsymbol{\sigma} = (\sigma_1^2, \dots, \sigma_d^2)$ such that $\frac{\mu_i - \nu_i}{\sigma_i} = c_i d^{-\alpha}$, $i = 1, \dots, d$, with $0 < \inf_i |c_i| \leq \sup_i |c_i| < +\infty$ and $\alpha > 0$, then:

$$\Pr_{\max}(p, q) \asymp \begin{cases} \frac{d^{\alpha-\frac{1}{2}}}{\sqrt{\pi} \bar{c}_d} \exp\left(-\frac{\bar{c}_d^2}{\sqrt{2}} d^{-2\alpha+1}\right) & \text{for } 0 < \alpha \leq \frac{1}{2} \\ 1 - \frac{2\bar{c}_d}{\sqrt{\pi}} d^{-\alpha+\frac{1}{2}} & \text{for } \alpha > \frac{1}{2} \end{cases} \quad \text{as } d \rightarrow \infty,$$

$$\prod_{i=1}^d \Pr_{\max}(p_i, q_i) \asymp \exp(-d^{1-\alpha} \tilde{c}_d) \quad \text{as } d \rightarrow \infty,$$

where $\bar{c}_d := \sqrt{\frac{\sum_{i=1}^d c_i^2}{8d}}$, $\tilde{c}_d = \frac{\sum_{i=1}^d |c_i|}{d\sqrt{2\pi}}$ and we write $f(x) \asymp g(x)$ whenever $\lim_{x \rightarrow +\infty} \frac{f(x)}{g(x)} = 1$

It follows that both probabilities go to zero for $0 < \alpha < 0.5$ as $d \rightarrow +\infty$, while for $0.5 < \alpha < 1$ only $\Pr_{\max}(p, q)$ goes to 1. For $\alpha > 1$, both probabilities converge to 1 (although with different regimes). In Figure 5 we report the ratio of the blocked and the component-wise meeting probabilities, i.e. $\Pr_{\max}(p, q) / (\prod_{i=1}^d \Pr_{\max}(p_i, q_i))$, for a d -dimensional Gaussian distribution with independent components, where $c_i = 1$ for all i and different values of α , along with a dotted line representing the value 1. Figure 5 shows that for $\alpha > 1$, the blocked maximal

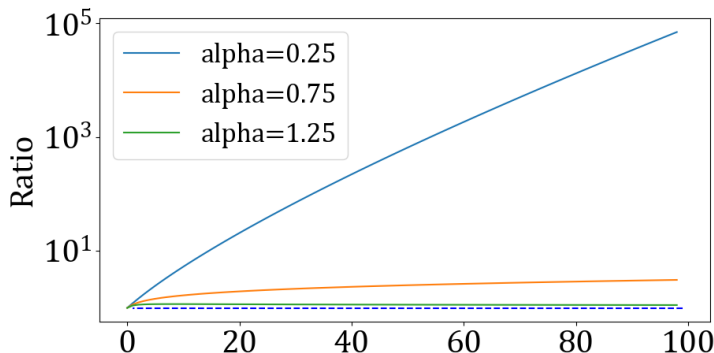


Figure 5: Ratio of blocked and component-wise meeting probability for d -dimensional Gaussian, different α values. Dimension on x -axis, logarithmic scale on y -axis.

coupling has meeting probabilities comparable to that of the independent counterpart.

7 High-dimensional GLMMs with crossed effects

We now consider applications to Model 2. First, Section 7.1 reviews state-of-the-art samplers and their computational cost for this class of models, and briefly discusses our coupling strategy, which requires to extend some of the methodologies of Section 6 to the case of Metropolis-within-Gibbs algorithms. Then Section 7.2 reports experimental results on simulated data.

7.1 Algorithms for Model 2

Similarly to what seen for Model 1 in Section 2.2, also for Model 2 the vanilla Gibbs procedure, i.e. the one updating from the full conditionals $\mu, \mathbf{a}^{(1)}, \dots, \mathbf{a}^{(K)}, \boldsymbol{\tau}$, suffers from slow mixing

because of the posterior correlation among the unknown random effects. Given the impossibility of analytically integrating out the global mean, [Papaspiliopoulos et al. \(2023\)](#) propose to perform at each iteration a $\mathcal{L}(\mu, \mathbf{a}^{(k)} | \mathbf{y}, \boldsymbol{\tau}, \mathbf{a}^{(-k)})$ -invariant update using local centering within each block, hence updating a new pair of variables $(\mu, \boldsymbol{\xi}^{(k)})$, where $\boldsymbol{\xi}^{(k)} := \mu + \mathbf{a}^{(k)}$. For the re-parametrized model it holds that $\mathcal{L}(\mu | \mathbf{a}^{(-k)}, \boldsymbol{\xi}^{(k)}, \boldsymbol{\tau}, \mathbf{y}) = \mathcal{L}(\mu | \boldsymbol{\xi}^{(k)})$ and that the $\boldsymbol{\xi}^{(k)}$ are conditionally independent, although their full conditional might not be available in closed form. In such cases one can replace exact Gibbs updates of $\boldsymbol{\xi}^{(k)}$ with more general invariant Markov updates. The resulting scheme is described in [Algorithm 3](#).

Algorithm 3: One iteration of Metropolis-within-Gibbs sampler with local centering for [Model 2](#)

```

for  $k=1, \dots, K$  do
  reparametrize  $(\mu, \mathbf{a}^{(k)}) \rightarrow (\mu, \boldsymbol{\xi}^{(k)})$ 
  draw  $\mu$  from  $\mathcal{L}(\mu | \boldsymbol{\xi}^{(k)})$ 
  for  $i=1, \dots, I_k$  do
    update  $\xi_i^{(k)}$  with a  $\mathcal{L}(\xi_i^{(k)} | \mu, \mathbf{a}^{(-k)}, \boldsymbol{\tau}, \mathbf{y})$ -invariant Markov kernel
  reparametrize  $(\mu, \boldsymbol{\xi}^{(k)}) \rightarrow (\mu, \mathbf{a}^{(k)})$ 
  draw  $\tau_k$  from  $\mathcal{L}(\tau_k | \mu, \mathbf{a}, \mathbf{y})$ 

```

For Gaussian targets and fixed $\boldsymbol{\tau}$, [Corollary 1](#) in [Papaspiliopoulos et al. \(2023\)](#) shows that

$$T_{cg} < T_{lc} < T_{cg} + C, \quad (17)$$

where T_{cg} and T_{lc} denote the relaxation times of [Algorithms 2](#) and [Algorithm 3](#), respectively, and C is a constant depending only on $\boldsymbol{\tau}$. The previous inequality allows to directly extend the results developed in [Section 5.2](#) for the collapsed Gibbs scheme to the local centering version in [Algorithm 3](#). Although the inequality holds only for Gaussian targets, numerical results in [Papaspiliopoulos et al. \(2023\)](#) show that also in the non conjugate case, where sampling of $\xi_i^{(k)}$ is done through Metropolis-Hastings updates, the convergence speed remains bounded as N and the number of parameters increase.

Remark 4 (Couplings of Metropolis-Hastings). Analogously to [\(15\)](#), $\mathcal{L}(\boldsymbol{\xi}^{(k)} | \mu, \mathbf{a}^{(-k)}, \boldsymbol{\tau}, \mathbf{y})$ factorizes as $\prod_{i=1}^{I_k} \mathcal{L}(\xi_i^{(k)} | \mu, \mathbf{a}^{(-k)}, \boldsymbol{\tau}, \mathbf{y})$. The difference is that $\mathcal{L}(\xi_i^{(k)} | \mu, \mathbf{a}^{(-k)}, \boldsymbol{\tau}, \mathbf{y})$ are not available in closed form and thus we update each $\xi_i^{(k)}$ with a MH step in [Algorithm 3](#). Similarly to [Section 6.2](#), leveraging conditional independence in the coupling of the MH kernels allows to have meeting times that grow at most logarithmically with I_k , see [Section B](#) in the supplement for details. In the MH case, however, there is additional flexibility ([Wang et al., 2021](#)), such as deciding how to couple both the proposal and acceptance steps as well as which of those to factorize. In [Section B](#) in the supplement, we discuss these aspects in some detail, suggesting to use a fully factorized strategy both on the proposal and acceptance. Also, due to the computational difficulty of efficiently implementing W_2 -optimal couplings of MH, we avoid the two step strategy of [Algorithm 1](#) and rather use a one-step approach for those updates, see again [Section B](#) in the supplement.

7.2 Numerical results

We apply the methodology discussed above to Model 2 and compare its performances with state-of-the-art black-box sampling algorithms such as the No-U-Turn-Sampler (NUTS) (Hoffman and Gelman, 2014) implemented in the popular software STAN (Carpenter et al., 2017). Note that the latter approach does not specifically use the structure of Model 2 and thus might be expected to be sub-optimal for that reason.

We simulate data from Model 2 with $K = 2$ factors, for Laplace response $\mathcal{L}(y_n|\mu, \mathbf{a}) = \text{Lapl}(\mu + a_{i_1[n]}^{(1)} + a_{i_2[n]}^{(2)}, 1)$ and $\tau_1 = \tau_2 = 1$, for Regime 2 of Section 5.3. We implement the Metropolis-within-Gibbs (MwG) scheme of Algorithm 3 with Random Walk Metropolis (RWM) updates. As for the coupling, in light of the results of Section B in the supplement, we implement Algorithm 8, with Gaussian proposals $Q(\mathbf{x}, d\mathbf{x}')$ coupled via maximal independent coupling (Algorithm 5), and paired acceptance. We report below the graph of the resulting average of the meeting times for different numbers of RWM steps within each iteration ($S = 1, 3$). It can

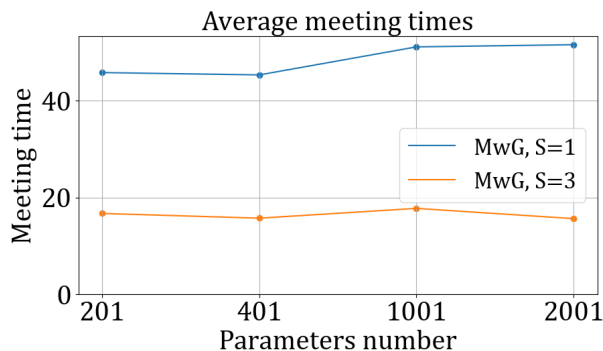


Figure 6: Estimated mean meeting times for $K = 2$, $I_1 = I_2 = I \in \{100, 200, 500, 1000\}$, $\tau_1 = \tau_2 = 1, b = 1$ with Laplace response. Algorithm 3 with different number of Metropolis steps S .

be noted from Figure 6 that the average of the meeting times remains almost constant as the number of parameters grows. Furthermore, the higher the number of Metropolis steps S within each iteration, the smaller the meeting time. Intuitively, as S grows, the conditional updates get closer to exact Gibbs updates and the resulting chain converges faster, leading to smaller meeting times. To put into context the performances of our estimation procedure, we illustrate in Figure 7 the convergence speed of the STAN implementation (Carpenter et al., 2017) of NUTS with the default setting, for estimating the same model. Specifically, we report the average number of gradient evaluations per Effective Sample Size (ESS), considering the minimum ESS across parameters. As Figure 6 and Figure 7 show, the $O(1)$ scaling of the meeting times of the MwG sampler with local centering as N and p diverge results in a $O(1)$ number of full likelihood evaluations per unbiased estimate, while a black-box method such as NUTS requires a number of gradient evaluations growing with p .

8 Probabilistic matrix factorization

Finally, we consider Model 3. A well-known feature of such model is that, for fixed \mathbf{u} , the model reduces to a standard linear regression with coefficients \mathbf{v} , and viceversa for fixed \mathbf{v} . On the

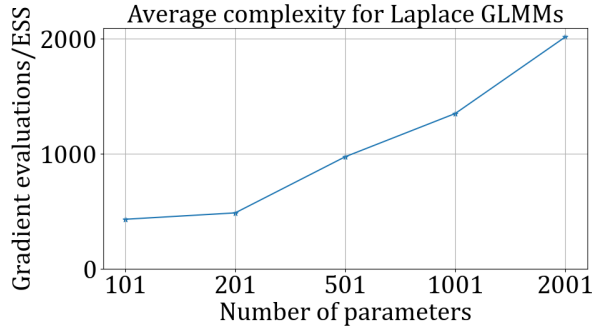


Figure 7: Average number of gradient evaluations divided by ESS (minimum across parameters) for NUTS, for $K = 2$, $I_1 = I_2 = I \in \{50, 100, 250, 500, 1000\}$, $\tau_1 = \tau_2 = 1$, $b = 1$ with Laplace response.

contrary, the likelihood is not analytically tractable if \mathbf{u} and \mathbf{v} vary jointly. As mentioned in Section 2, this structure naturally lends itself to conditional updating schemes, such as BGS for sampling or block coordinate ascent (usually called alternating least squares whenever applied to Model 3) for optimization. However, the vanilla BGS scheme, which updates \mathbf{u} , \mathbf{v} , ρ , $\boldsymbol{\tau}$ from their full conditionals at every iteration, often results in slow mixing of the chain, for reasons analogous to the ones discussed for Models 1 and 2 in previous sections (see also numerics in Figure 8). We thus propose a “local centering” version of BGS for Model 3, where we reparametrise the random effects using ρ , i.e. at each iteration we update $(\rho, \bar{\mathbf{u}})$, with $\bar{\mathbf{u}} := \rho\mathbf{u}$, and then $(\rho, \bar{\mathbf{v}})$, for $\bar{\mathbf{v}} := \rho\mathbf{v}$ analogously. Algorithm 4 provides high-level pseudo-code for one iteration of the resulting scheme, while Algorithm 9 in the supplement provides full implementation details.

Algorithm 4: One iteration of BGS with local centering for Model 3

```

for  $(\mathbf{r}, \mathbf{s}) \in \{(\mathbf{u}, \mathbf{v}), (\mathbf{v}, \mathbf{u})\}$  do
  reparametrize  $(\rho, \mathbf{r}) \rightarrow (\rho, \bar{\mathbf{r}})$ , with  $\bar{\mathbf{r}} := \rho\mathbf{r}$ 
  draw  $\rho \sim \mathcal{L}(\rho|\bar{\mathbf{r}}, \mathbf{s}, \tau_0, \mathbf{y})$ 
  draw  $\bar{\mathbf{r}} \sim \mathcal{L}(\bar{\mathbf{r}}|\rho, \mathbf{s}, \tau_0, \mathbf{y})$ 
  reparametrize  $(\rho, \bar{\mathbf{r}}) \rightarrow (\rho, \boldsymbol{\tau})$ 
draw  $\tau_0 \sim \mathcal{L}(\tau_0|\rho, \mathbf{u}, \mathbf{v}, \mathbf{y})$ 

```

Regarding the UMCMC version of Algorithm 4, since the high-dimensional full conditionals involved are multivariate Gaussian, we can implement the same coupling strategy as for Model 1, namely Algorithmic specification 2. In particular, joint maximal couplings for the high-dimensional updates of $\bar{\mathbf{r}}$ can be implemented efficiently. Below we provide numerical illustrations of the performances of the UMCMC version of Algorithm 4 and vanilla BGS. As discussed in more details in Remark 6, we restrict ourselves to the case $d = 1$.

Remark 5 (Related literature on Bayesian factor models). Model 3 is closely related to Bayesian factor analysis. With the same notation as in (3), a factor model (Gorsuch, 2014) can be written as

$$y_n | \boldsymbol{\mu}, \mathbf{F}, \Lambda, \boldsymbol{\tau} \sim N(\mu_{i[n]} + \Lambda_{j[n],:} \mathbf{F}_{i[n]}, \tau_0^{-1}), \quad (18)$$

for $\boldsymbol{\mu} \in \mathbb{R}^{I_1}$, $\mathbf{F} = (\mathbf{F}_i)_{i=1}^{I_1}$ being the collection of unknown factors, $\mathbf{F}_i \in \mathbb{R}^d$, and $\Lambda \in \mathbb{R}^{I_2 \times d}$ the factor loading matrix, with d being the latent dimension. Indeed, factor models exhibit the same structure of Model 3, and BGS schemes are also widely used in that context (Conti et al.,

2014; Papastamoulis and Ntzoufras, 2022), even if there the focus is usually on the full design case (where all the combinations users/films are observed) and on regimes where $I_2 \ll I_1$ and I_1 grows.

Remark 6 (Issues related to rotational invariance). A well-known issue of Model 3 is the invariance with respect to joint rotations of \mathbf{u} and \mathbf{v} . This creates multimodality in the posterior, thus inducing slow convergence and lack of posterior interpretability. Many ad hoc methodologies have been developed to deal with such issue, including constraining a priori the matrix of factor loadings or post-processing (Conti et al., 2014; Papastamoulis and Ntzoufras, 2022). Although of interest, these issues and techniques are somehow orthogonal to our focus here, and thus we restrict to the case $d = 1$ for simplicity and leave further exploration to future work.

8.1 Numerical results

We simulate data coming from Model 3 for different asymptotic regimes and parameter specifications. We consider $I_1 = I_2 = I \in \{100, 200, 500, 1000\}$ levels and data coming from Regime 1 and 2. In Figure 8 we report the average meeting times for both vanilla BGS (PV in the legend) and Algorithm 4 (Local Centering) with Algorithmic specification 2 as discussed above. As expected, the slow mixing of vanilla BGS results in exploding meeting times of the coupled

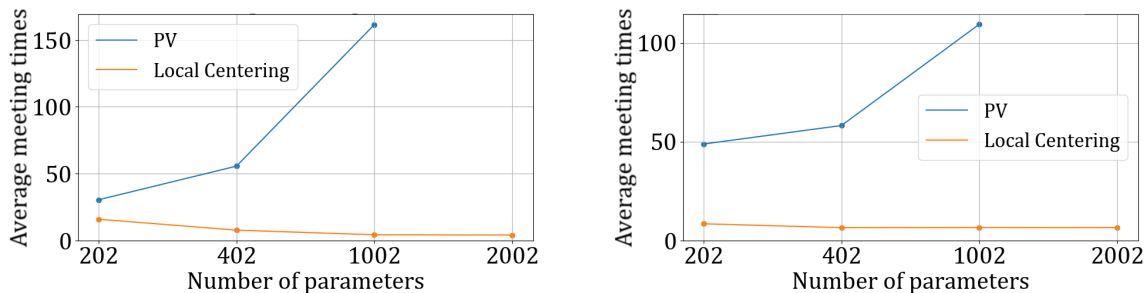


Figure 8: Estimated mean meeting times for Probabilistic Matrix Factorization model. $I_1 = I_2 = I \in \{100, 20, 500, 1000\}$. Left: Regime 1, right: Regime 2.

chains, which are not reported for I greater than 500 for visual convenience. Remarkably, as few as 10 iterations are on average sufficient for the coupled chains evolving according to Algorithm 4 to meet even in the high-dimensional cases.

9 Conclusion

Building on the recent advancements presented in Jacob et al. (2020) and Papaspiliopoulos et al. (2019, 2023), we propose a UMCMC procedure specifically tailored for high-dimensional BGS with high degree of conditional independence. In the Gaussian case, we show the resulting expected meeting times are bounded by a quantity that depends on the relaxation time of the individual chains, multiplied by its logarithm. In several applications, this results in procedures that require as few as a dozen iterations to obtain unbiased estimates for complex models with over 10,000 parameters, thus enhancing the appeal of efficient and cost-effective parallelization.

Interestingly, unlike many sampling algorithms (such as gradient-based ones), no adaptation of tuning parameters is required for BGS. This couples particularly well with the UMCMC

framework: specifically, it avoids the need for potentially long preliminary runs or adaptation phases, thus genuinely allowing for parallelizable short runs and "early stopping" in case of fast mixing chains, see also [Biswas et al. \(2022\)](#) for analogous examples.

We conclude by mentioning some possible directions for future research. First, while challenging, it would be valuable to extend the theoretical results of Section 4 beyond the Gaussian case. A possible approach would be to leverage the recent results on BGS for log-concave distributions in [Ascolani et al. \(2024\)](#). More generally, it is relevant to assess which coupling methodologies lead to meeting times that are of the same order of mixing or relaxation times of the original chain, similarly to Theorems 1, 2 and 3. As discussed in Remark 2, we expect the results in Section 4 to extend relatively directly to control higher moments of T , thus implying finite variance of the unbiased estimator ([Atchadé and Jacob, 2024](#), Thm.2.1). Also, it would be interesting to derive lower bounds for the average meeting times of coupled chains explicitly depending on the convergence properties of the original chain, in order to make the arguments of Section 4.2 rigorous. Finally, on a different line of research, an interesting direction could be to provide a broader analysis and development of local centering schemes for probabilistic matrix factorization (PMF).

Funding

GZ acknowledges support from the European Research Council (ERC), through StG "PrSc-HDBayLe" grant ID 101076564.

References

- Beskos Alexandros and Gareth O. Roberts. One-Shot CFTP, Application to a Class of Truncated Gaussian Densities. *Methodology and Computing in Applied Probability*, 76(1):407–437, 2005.
- Filippo Ascolani, Hugo Lavenant, and Giacomo Zanella. Entropy contraction of the Gibbs sampler under log-concavity. *Preprint at <https://arxiv.org/pdf/2410.00858>*, 2024.
- Yves F. Atchadé and Pierre E. Jacob. Unbiased Markov Chain Monte Carlo: what, why, and how. *Preprint at <https://arxiv.org/html/2406.06851v1>*, 2024.
- Rolf H Baayen, Douglas J Davidson, and Douglas M Bates. Mixed-effects modeling with crossed random effects for subjects and items. *Journal of memory and language*, 59(4):390–412, 2008.
- Douglas Bates, Martin Mächler, Ben Bolker, and Steve Walker. Fitting linear mixed-effects models using lme4. *Journal of Statistical Software*, 67(1):1–48, 2015.
- Niloy Biswas, Pierre E. Jacob, and Paul Vanetti. Estimating convergence of Markov chains with L-lag couplings. *Advances in neural information processing systems*, pages 7389–7399, 2019.
- Niloy Biswas, Anirban Bhattacharya, Pierre Jacob, and James Johndrow. Coupling-based convergence assessment of some Gibbs samplers for high-dimensional Bayesian regression with shrinkage priors. *Journal of the Royal Statistical Society: Series B (Statistical Methodology)*, 84, 03 2022.

- Nawaf Bou-Rabee, Andreas Eberle, and Raphael Zimmer. Coupling and convergence for Hamiltonian Monte Carlo. *The Annals of Applied Probability*, 30(3):1209 – 1250, 2020a.
- Nawaf Bou-Rabee, Andreas Eberle, and Raphael Zimmer. Coupling and convergence for Hamiltonian Monte Carlo. *The Annals of Applied Probability*, 30(3):1209 – 1250, 2020b.
- Yann Brenier. Polar factorization and monotone rearrangement of vector-valued functions. *Communications on Pure and Applied Mathematics*, 44(4):375–417, 1991.
- Gerandy Brito, Ioana Dumitriu, and Kameron Decker Harris. Spectral gap in random bipartite biregular graphs and applications. *Comb. Probab. Comput.*, 31:229–267, 2018.
- Bob Carpenter, Andrew Gelman, Matthew D. Hoffman, Daniel Lee, Ben Goodrich, Michael Betancourt, Marcus Brubaker, Jiqiang Guo, Peter Li, and Allen Riddell. Stan: A Probabilistic Programming Language. *Journal of Statistical Software*, 76(1):1–32, 2017.
- Gabriella Conti, Sylvia Frühwirth-Schnatter, James J. Heckman, and Remi Piatek. Bayesian exploratory factor analysis. *Journal of Econometrics*, 183(1):31–57, 2014.
- José R. Correa and Matías Romero. On the asymptotic behavior of the expectation of the maximum of i.i.d. random variables. *Operations Research Letters*, 49(5):785–786, 2021.
- D. C. Dowson and B. V. Landau. The Fréchet distance between multivariate normal distributions. *J. Multivariate Anal.*, 12(3):450–455, 1982.
- Andreas Eberle, Arnaud Guillin, and Raphael Zimmer. Couplings and quantitative contraction rates for Langevin dynamics. *The Annals of Probability*, 47(4):1982 – 2010, 2019.
- Katelyn Gao and Art Owen. Efficient moment calculations for variance components in large unbalanced crossed random effects models. *Electronic Journal of Statistics*, 11, 01 2016.
- Izrail Gelfand. Normierte ringe. *Rec. Math. [Mat. Sbornik] N.S.*, 9(51)(1):3–24, 1941.
- Andrew Gelman. Analysis of Variance: Why It Is More Important than Ever. *Annals of Statistics*, pages 1–31, 2005.
- Andrew Gelman and Jennifer Hill. *Data Analysis Using Regression and Multilevel/Hierarchical Models*. Analytical Methods for Social Research. Cambridge University Press, 2006.
- Swarnadip Ghosh, Trevor J. Hastie, and Art B. Owen. Backfitting for large scale crossed random effects regressions. *The Annals of Statistics*, 2022.
- Clark R. Givens and Rae Michael Shortt. A class of Wasserstein metrics for probability distributions. *Michigan Mathematical Journal*, 31(2):231 – 240, 1984.
- Peter W. Glynn and Chang-Han Rhee. Exact estimation for Markov chain equilibrium expectations. *Journal of Applied Probability*, 51(A):377–389, 2014.
- Richard L. Gorsuch. *Factor Analysis: Classic Edition (2nd ed.)*. Routledge, 2014.
- David Griffeath. A maximal coupling for Markov chains. *Zeitschrift für Wahrscheinlichkeitstheorie und Verwandte Gebiete*, 31(2):95–106, 1975.

- Matthew D Hoffman and Andrew Gelman. The No-U-Turn sampler: adaptively setting path lengths in Hamiltonian Monte Carlo. *J. Mach. Learn. Res.*, 15(1):1593–1623, 2014.
- Pierre E. Jacob, John O’Leary, and Yves F. Atchadé. Unbiased Markov chain Monte Carlo methods with couplings. *Journal of the Royal Statistical Society: Series B (Statistical Methodology)*, 82(3):543–600, 2020.
- Jiming Jiang and Thuan Nguyen. *Linear and Generalized Linear Mixed Models and Their Applications*. 2021.
- Kshitij Khare and Hua Zhou. Rates of convergence of some multivariate Markov chains with polynomial eigenfunctions. *Annals of Applied Probability*, 19:737–777, 2009.
- Herbert Knothe. Contributions to the theory of convex bodies. *Michigan Mathematical Journal*, 4(1):39–52, 1957.
- David A. Levin and Yuval Peres. *Markov chains and mixing times*, volume 107. American Mathematical Soc., 2017.
- Marianne Menictas, Gioia Di Credico, and Matt P Wand. Streamlined variational inference for linear mixed models with crossed random effects. *Journal of Computational and Graphical Statistics*, 32(1):99–115, 2023.
- Lawrence Middleton, George Deligiannidis, Arnaud Doucet, and Pierre E. Jacob. Unbiased Markov chain Monte Carlo for intractable target distributions. *Electronic Journal of Statistics*, 14(2):2842 – 2891, 2020.
- Jeffrey W. Miller and Scott L. Carter. Inference in generalized bilinear models. *Preprint at <https://arxiv.org/abs/2010.04896>*, 2020.
- Ingram Olkin and Friedrich Pukelsheim. The distance between two random vectors with given dispersion matrices. *Linear Algebra Appl.*, 48:257–263, 1982.
- Andrea Pandolfi, Omiros Papaspiliopoulos, and Giacomo Zanella. Conjugate gradient methods for high-dimensional GLMMs. *in preparation*, 2024.
- Omiros Papaspiliopoulos, Gareth O. Roberts, and Giacomo Zanella. Scalable inference for crossed random effects models. *Biometrika*, 107(1):25–40, 11 2019.
- Omiros Papaspiliopoulos, Timothée Stumpf-Fétizon, and Giacomo Zanella. Scalable Bayesian computation for crossed and nested hierarchical models. *Electronic Journal of Statistics*, 17(2):3575 – 3612, 2023.
- Panagiotis Papastamoulis and Ioannis Ntzoufras. On the identifiability of Bayesian factor analytic models. *Statistics and Computing*, 32(23), 2022.
- Tamás P. Papp and Chris Sherlock. A new and asymptotically optimally contracting coupling for the random walk Metropolis. *Preprint at <https://arxiv.org/abs/2211.12585>*, 2022.
- Patrick O Perry. Fast moment-based estimation for hierarchical models. *Journal of the Royal Statistical Society Series B: Statistical Methodology*, 79(1):267–291, 2017.

- Gareth O. Roberts and Jeffrey S. Rosenthal. One-shot coupling for certain stochastic recursive sequences. *Stochastic Processes and their Applications*, 99(2):195–208, 2002.
- Gareth O. Roberts and Sujit K. Sahu. Updating Schemes, Correlation Structure, Blocking and Parameterization for the Gibbs Sampler. *Journal of the Royal Statistical Society. Series B (Methodological)*, 59(2):291–317, 1997.
- Gareth O. Roberts, Andrew Gelman, and W. R. Gilks. Weak Convergence and Optimal Scaling of Random Walk Metropolis Algorithms. *The Annals of Applied Probability*, 7(1):110–120, 1997.
- Murray Rosenblatt. Remarks on a multivariate transformation. *The annals of mathematical statistics*, 23(3):470–472, 1952.
- Jeffrey S. Rosenthal. Asymptotic Variance and Convergence Rates of Nearly-Periodic Markov Chain Monte Carlo Algorithms. *Journal of the American Statistical Association*, 98(461):169–177, 2003.
- Ruslan Salakhutdinov and Andriy Mnih. Bayesian probabilistic matrix factorization using Markov chain Monte Carlo. volume 25, pages 880–887, 01 2008.
- Filippo Santambrogio. *Optimal transport for applied mathematicians*. 2015.
- Hermann Thorisson. *Coupling, Stationarity, and Regeneration*. Springer, 2000.
- Guanyang Wang, John O’Leary, and Pierre Jacob. Maximal Couplings of the Metropolis-Hastings Algorithm. *Proceedings of The 24th International Conference on Artificial Intelligence and Statistics, PMLR*, pages 1225–1233, 2021.
- Simon Wood. *Generalized Additive Models: An Introduction with R, Second Edition (2nd ed.)*. Chapman and Hall/CRC, 2017.

A Background on couplings

A.1 Maximal Coupling Algorithms

We briefly review algorithms for sampling from maximal couplings of two distributions $p, q \in \mathcal{P}(\mathcal{X})$, with $\mathcal{X} = \mathbb{R}^d$. Provided p and q admit densities, there always exists an algorithm with maximal meeting probability (Thorisson, 2000, Sec. 4.5 of Chap 1), referred to as *maximal rejection* (Algorithm 5). However, in the case of spherically symmetric distributions (e.g. multivariate Gaussian with the same covariance matrix), an alternative approach called *maximal reflection coupling* (see Algorithm 6 or (Eberle et al., 2019; Bou-Rabee et al., 2020b)) allows for sampling with a deterministic cost and yet allowing for a good contraction of the square distance between the resulting draws (see e.g. Lemma 2).

Maximal rejection coupling. Algorithm 5 reports the pseudo code for implementing a maximal rejection coupling of p, q . The computational cost of Algorithm 5 depends on the number of

Algorithm 5: Maximal rejection coupling of $p, q \in \mathcal{P}(\mathbb{R}^d)$

```

sample  $\mathbf{X} \sim p$ 
sample  $W \sim U(0, 1)$ 
if  $Wp(\mathbf{X}) \leq q(\mathbf{X})$  then
   $\perp$  set  $\mathbf{Y} = \mathbf{X}$ 
else
  sample  $\mathbf{Y}^* \sim q$  and  $W^* \sim U(0, 1)$ 
  while  $W^*q(\mathbf{Y}^*) < p(\mathbf{Y}^*)$  do
     $\perp$  sample  $\mathbf{Y}^* \sim q$  and  $W^* \sim U(0, 1)$ 
   $\perp$  set  $\mathbf{Y} = \mathbf{Y}^*$ 

```

iterations required to accept the proposed sample. Only one sample is required if \mathbf{X} is accepted as value for \mathbf{Y} , and this happens with probability $\Pr(p(\mathbf{X})W \leq q(\mathbf{X})) = 1 - \|p - q\|_{TV}$. If instead \mathbf{X} is rejected, the number of trials before acceptance follows a Geometric variable with parameter $\Pr(q(\mathbf{Y}^*)W^* > p(\mathbf{Y}^*))$, the latter being equal to $\|p - q\|_{TV}$. The resulting expected number of iterations is

$$1 - \|p - q\|_{TV} + \|p - q\|_{TV}(1/\|p - q\|_{TV} + 1) = 2.$$

The variance of the expected number of iterations is equal to $\frac{2(1 - \|p - q\|_{TV})}{\|p - q\|_{TV}}$, which tends to infinity as $\|p - q\|_{TV}$ approaches zero. Gerber and Lee proposed accepting the first draw with a lower probability, thereby avoiding the problem of infinite variance, but at the cost of losing maximality (see the discussion in Jacob et al. (2020)).

Maximal reflection coupling. Algorithm 6 reports an implementation of maximal reflection coupling for Gaussian distributions with same covariance matrix. Note that, differently from Algorithm 5, in Algorithm 6 no rejection mechanism is required and the algorithm's runtime is deterministic. Furthermore, in high-dimensional cases, this procedure shows favourable behaviours: in addition to being maximal, the algorithm contracts the distance between chains with a good rate. Thus, when applicable, it is generally preferred to Algorithm 5.

Algorithm 6: Maximal reflection coupling of $N(\boldsymbol{\xi}, \Sigma)$ and $N(\boldsymbol{\nu}, \Sigma)$

```

set  $\mathbf{z} = \Sigma^{-1/2}(\boldsymbol{\xi} - \boldsymbol{\nu})$ ,  $\mathbf{e} = \mathbf{z}/\|\mathbf{z}\|$ 
sample  $\dot{\mathbf{X}} \sim N_d(\mathbf{0}, I_d)$ ,  $W \sim U(0, 1)$ 
if  $W \leq \exp\{-\frac{1}{2}\mathbf{z}^\top(2\dot{\mathbf{X}} + \mathbf{z})\}$  then
  | set  $\dot{\mathbf{Y}} = \dot{\mathbf{X}} + \mathbf{z}$ 
else
  |  $\dot{\mathbf{Y}} = \dot{\mathbf{X}} - 2(\mathbf{e}^\top \dot{\mathbf{X}})\mathbf{e}$ 
 $\mathbf{X} = \Sigma^{1/2}\dot{\mathbf{X}} + \boldsymbol{\xi}$ 
 $\mathbf{Y} = \Sigma^{1/2}\dot{\mathbf{Y}} + \boldsymbol{\nu}$ 

```

A.2 W_2 -optimal maps

For all univariate distributions, it is known that the *monotone map* coupling (i.e. using same random number for inverse cdf method) is optimal for every cost function of the form $c(x, y) = h(x - y)$ with h convex (Santambrogio, 2015, Thm.2.9), and hence is W_2 -optimal. For p, q univariate distributions, let $F_p(\cdot)$ and $F_q(\cdot)$ denote their cumulative density function (cdf). We define the inverse cdf as

$$F_p^{-1}(u) := \inf_{t \in \mathbb{R}} \{t : F_p(t) \geq u\},$$

and F_q^{-1} accordingly. It is then possible to sample from the W_2 optimal coupling as in Algorithm 7.

Algorithm 7: monotone transport map for univariate distributions

```

sample  $U \sim U(0, 1)$ 
set  $X = F_p^{-1}(U)$ 
set  $Y = F_q^{-1}(U)$ 

```

No universal optimality result exists for general multivariate distributions, but a natural extension of the monotone map above, called *common random number (crn)* coupling, is indeed optimal for multivariate Gaussians whose covariance matrices commute (Dowson and Landau, 1982; Olkin and Pukelsheim, 1982), as stated below. While the following result is known, we report a proof for self-containedness.

Lemma 6 (Optimality of *crn* coupling for Gaussian distributions). *Let $p = N(\boldsymbol{\xi}, \Sigma_1)$ and $q = N(\boldsymbol{\nu}, \Sigma_2)$ be d -dimensional Gaussian, with $\Sigma_1 \Sigma_2 = \Sigma_2 \Sigma_1$. Define*

$$\Gamma^* := N \left(\begin{pmatrix} \boldsymbol{\xi} \\ \boldsymbol{\nu} \end{pmatrix}, \begin{pmatrix} \Sigma_1 & FG^\top \\ GF^\top & \Sigma_2 \end{pmatrix} \right), \quad (19)$$

where $FF^\top = \Sigma_1, GG^\top = \Sigma_2$. Then $\Gamma^* \in \Gamma_{W_2}(p, q)$, i.e. Γ^* is the W_2 -optimal coupling of p and q .

Proof of Lemma 6. Let $(\mathbf{X}, \mathbf{Y}) \sim \Gamma^*$. If $\mathbf{Z} \sim N(\mathbf{0}, I_d)$, we have $\mathbf{X} \stackrel{d}{=} \boldsymbol{\xi} + F\mathbf{Z}$, $\mathbf{Y} \stackrel{d}{=} \boldsymbol{\nu} + G\mathbf{Z}$, where $FF^\top = \Sigma_1$ and $GG^\top = \Sigma_2$ and $\stackrel{d}{=}$ denotes equality in distribution. Denote the (i, j) -th

entry of F and G as f_{ij} and g_{ij} , respectively. It holds

$$\begin{aligned}\mathbb{E}[\|\mathbf{X} - \mathbf{Y}\|^2] &= \mathbb{E}[\|\boldsymbol{\xi} - \boldsymbol{\nu} + (F - G)\mathbf{Z}\|^2] = \sum_{i=1}^d \mathbb{E} \left[\left((\xi_i - \nu_i) + \sum_{j=1}^d (f_{ij} - g_{ij})Z_j \right)^2 \right] \\ &= \sum_{i=1}^d (\xi_i - \nu_i)^2 + \sum_{i=1}^d \mathbb{E} \left[\left(\sum_{j=1}^d (f_{ij} - g_{ij})Z_j \right)^2 \right] + 2 \sum_{i=1}^d (\xi_i - \nu_i) \left(\sum_{j=1}^d (f_{ij} - g_{ij})\mathbb{E}[Z_j] \right).\end{aligned}$$

Since $\mathbb{E}[Z_i] = 0$, $\mathbb{E}[Z_i Z_j] = 0$ for $i \neq j$ and $Z_j^2 \sim \chi(1)$, then

$$\begin{aligned}\mathbb{E}[\|\mathbf{X} - \mathbf{Y}\|^2] &= \|\boldsymbol{\xi} - \boldsymbol{\nu}\|^2 + \mathbb{E}[\|(F - G)\mathbf{Z}\|^2] \\ &= \|\boldsymbol{\xi} - \boldsymbol{\nu}\|^2 + \sum_{ij} |f_{ij} - g_{ij}|^2 = \|\boldsymbol{\xi} - \boldsymbol{\nu}\|^2 + \|F - G\|_{fr}^2,\end{aligned}$$

where $\|\cdot\|_{fr}$ denotes the Frobenius norm of matrices. The latter expression exactly equals the minimizer of the optimal transport problem in the Gaussian case, whenever the variance covariance matrices commute (Givens and Shortt, 1984). \square

Thus, in order to obtain draws from Γ^* in Lemma 6, one can simply sample $\mathbf{Z} \sim N(\mathbf{0}_d, \mathbf{1}_d)$ and then set

$$\begin{cases} \mathbf{X} = \boldsymbol{\mu} + F\mathbf{Z}, \\ \mathbf{Y} = \boldsymbol{\nu} + G\mathbf{Z}. \end{cases} \quad (20)$$

We will refer to (20) as *crn* coupling. Recall also that the W_2 -optimal map is unique (Brenier, 1991).

B Couplings for Metropolis-Hastings algorithms for product targets

In this section we discuss procedures for efficient coupling of Metropolis-Hastings (MH) kernels for targets with independent components. The motivation for such a construction stems from Algorithm 3 applied to Model 2, where each iteration consists of updating K blocks of (conditionally) independent coordinates, since each $\mathcal{L}(\boldsymbol{\xi}^{(k)} | \mu, \mathbf{a}^{-(k)}, \boldsymbol{\tau}, \mathbf{y})$ factorizes in $\prod_{i=1}^{I_k} \mathcal{L}(\xi_i^{(k)} | \mu, \mathbf{a}^{-(k)}, \boldsymbol{\tau}, \mathbf{y})$ for $k = 1, \dots, K$, whose distribution might be known only up to constants. Exploiting such independence in the coupling construction, one can derive coupling strategies whose meeting times grows logarithmically with I_k , see below. Previous works on couplings for MH kernels include Wang et al. (2021), where among other things the authors suggest employing a maximal reflection coupling on Gaussian proposals and paired acceptance, and Papp and Sherlock (2022), where the authors focus on asymptotically optimally contractive couplings.

Consider a target distribution ν on $\mathcal{X} = \mathbb{R}^{I_k}$ with independent components, i.e. $\nu = \otimes_{i=1}^{I_k} \nu_i$. The general Metropolis kernel targeting ν has the form

$$P_b^{MH}(\mathbf{x}, d\mathbf{x}') = Q_b(\mathbf{x}, d\mathbf{x}') a_b(\mathbf{x}, \mathbf{x}') + \delta_{\mathbf{x}}(d\mathbf{x}') r_b(\mathbf{x}), \quad (21)$$

where $Q_b(\mathbf{x}, d\mathbf{x}')$ denotes the proposal distribution on $\mathcal{X} = \mathbb{R}^{I_k}$, $a_b(\mathbf{x}, \mathbf{x}')$ is the Metropolis

acceptance ratio, i.e. $a_b(\mathbf{x}, \mathbf{x}') = 1 \wedge \frac{\nu(\mathbf{x}') Q_b(\mathbf{x}', \mathbf{x})}{\nu(\mathbf{x}) Q_b(\mathbf{x}, \mathbf{x}'')}$, and $r_b(\mathbf{x}) = 1 - \int_{\mathcal{X}} Q_b(\mathbf{x}, d\mathbf{x}') a_b(\mathbf{x}, d\mathbf{x}')$. The standard way to sample from P_b^{MH} in (21) is sampling a proposal \mathbf{x}' from $Q_b(\mathbf{x}, \cdot)$, compute $a_b(\mathbf{x}, \mathbf{x}')$ and accept if $U \sim U(0, 1)$ is smaller than the acceptance ratio. Given the known independence structure of the target, however, it is possible to propose and accept/reject each component individually, leading to much higher acceptance rates and better dimensionality scaling. The resulting kernel, which is a product of univariate MH kernels, can be written as

$$P_f^{MH}(\mathbf{x}, d\mathbf{x}') = \otimes_{i=1}^{I_k} P_i^{MH}(x_i, dx'_i) = \otimes_{i=1}^{I_k} (Q_f(x_i, dx'_i) a_f(x_i, x'_i) + \delta_{x_i}(dx'_i) r_f(x_i)), \quad (22)$$

where $Q_f(x_i, dx'_i)$ is a proposal kernel on \mathbb{R} , $a_f(x_i, x'_i) = 1 \wedge \frac{\nu_i(x'_i) Q_f(x'_i, x_i)}{\nu_i(x) Q_f(x_i, x'_i)}$, and analogously $r_f(x) = 1 - \int_{\mathbb{R}} Q_f(x_i, dx'_i) a_f(x_i, dx'_i)$. Note that (21) proposes and accept jointly all the components at once, while (22) does it component-wise. The coupling strategy can exploit such independence in two different ways, namely factorizing both the proposal and acceptance step or only the acceptance step.

Differently from models with conjugate full-conditional distributions (such as e.g. Models 1 and 3), (optimally) contractive couplings for MH kernels are difficult to implement, requiring numerical integration, and in our simulations they did not provide significant enough decrease in distance within subsequent steps to justify their use. Similarly, simple *crn* couplings of the MH kernels, i.e. using same random number for the proposal distributions (amounting at implementing the W_2 optimal coupling on the proposals whenever Gaussians) and acceptance steps, were also not effective in contracting efficiently the chains (specifically they typically soon reach a plateau distance not small enough to provide high chances of coalescence). For the above reasons, when using MH steps to update from high-dimensional and conditionally independent blocks, we avoid the two step strategy of Algorithm 1 and instead concentrate on one-step, maximal-only strategies.

Following guidelines in Wang et al. (2021), we consider kernels with synchronous acceptance, i.e. using same uniform for accept-reject in the \mathbf{x} and \mathbf{y} chain. For a_b, a_f, r_b and r_f as in (21) and (22), we define

$$\begin{aligned} \bar{a}_b &= \begin{pmatrix} a_b(\mathbf{x}, \mathbf{x}') \cdot \mathbf{1}_{I_k} \\ a_b(\mathbf{y}, \mathbf{y}') \cdot \mathbf{1}_{I_k} \end{pmatrix} \in \mathbb{R}^{2I_k}, & \bar{a}_f &= \begin{pmatrix} a_f(x_i, x'_i) \\ a_f(y_i, y'_i) \end{pmatrix} \in \mathbb{R}^2, \\ \Delta_b &= \begin{pmatrix} \delta_{\mathbf{x}}(d\mathbf{x}') r_b(\mathbf{x}) \\ \delta_{\mathbf{y}}(d\mathbf{y}') r_b(\mathbf{y}) \end{pmatrix} \in \mathbb{R}^{2I_k}, & \Delta_f &= \begin{pmatrix} \delta_{x_i}(dx'_i) r_f(x_i) \\ \delta_{y_i}(dy'_i) r_f(y_i) \end{pmatrix} \in \mathbb{R}^2, \end{aligned}$$

where $\mathbf{1}_{I_k}$ denotes the vector of ones of length I_k . Below we illustrate numerically the performances of the following list of possible coupled kernels:

1. *Blocked reflection*: $\bar{P}_{b,r} := \bar{P}_{max}[Q_b] \odot \bar{a}_b + \Delta_b$, where $\bar{P}_{max}[Q_b]$ is Algorithm 6 and \odot denotes the Hadamard product, i.e. component-wise product.
2. *Blocked maximal*: $\bar{P}_{b,m} := \bar{P}_{max}[Q_b] \odot \bar{a}_b + \Delta_b$, where $\bar{P}_{max}[Q_b]$ is Algorithm 5.
3. *Blocked factorized reflection*: $\bar{P}_{bf,r} := \otimes_{i=1}^{I_k} (\bar{P}_{max}[Q_b]_{[i]} \odot \bar{a}_f + \Delta_f)$, where, if $(\mathbf{x}, \mathbf{y}) \sim \bar{P}_{max}[Q_b]$, the symbol $\bar{P}_{max}[Q_b]_{[i]}$ indicates the vector (x_i, y_i) , and $\bar{P}_{max}[Q_b]$ is Algorithm 6.
4. *Blocked factorized maximal*: $\bar{P}_{bf,m} := \otimes_{i=1}^{I_k} (\bar{P}_{max}[Q_b]_{[i]} \odot \bar{a}_f + \Delta_f)$, where $\bar{P}_{max}[Q_b]$ is

Algorithm 5.

5. *Fully factorized reflection*: $\bar{P}_{ff,r} := \otimes_{i=1}^{I_k} (\bar{P}_{max}[Q_f] \odot \bar{a}_f + \Delta_f)$, where $\bar{P}_{max}[Q_b]$ is Algorithm 6.
6. *Fully factorized maximal*: $\bar{P}_{ff,m} := \otimes_{i=1}^{I_k} (\bar{P}_{max}[Q_f] \odot \bar{a}_f + \Delta_f)$, where $\bar{P}_{max}[Q_b]$ is Algorithm 5.

We report in Algorithm 8 the pseudo-code for one iteration of either $\bar{P}_{bf,r}$, $\bar{P}_{bf,m}$, $\bar{P}_{ff,r}$ or $\bar{P}_{ff,m}$, depending on the specification of $\bar{P}[Q]$.

Algorithm 8: Coupling strategy for MH with independent target

Input: $(\mathbf{X}^t, \mathbf{Y}^t)$, target ν , proposal Q , desired coupling \bar{P}
sample $(\mathbf{X}', \mathbf{Y}') \sim \bar{P}[Q]((\mathbf{X}^t, \mathbf{Y}^t), \cdot)$ **for** $i = 1, \dots, I_k$ **do**
 sample $U \sim U(0, 1)$ **if** $U \leq \frac{\nu(X'_i) Q(X'_i, X_i^t)}{\nu(X_i^t) Q(X_i^t, X'_i)}$ **then**
 | set $X_i^{t+1} = X'_i$
 else
 | set $X_i^{t+1} = X_i^t$
 if $U \leq \frac{\nu(Y'_i) Q(Y'_i, Y_i^t)}{\nu(Y_i^t) Q(Y_i^t, Y'_i)}$ **then**
 | set $Y_i^{t+1} = Y'_i$
 else
 | set $Y_i^{t+1} = Y_i^t$
 | $t = t + 1$

We provide a numerical illustration where ν is taken to be a product of independent Laplace distributions, i.e. $\nu = \otimes_{i=1}^d \text{Lapl}(0, 1/\sqrt{2})$. Consider $(\mathbf{X}^t, \mathbf{Y}^t)_{t \geq 0}$ coupled chains marginally evolving via the kernels 1 to 6 above with $Q_b(\mathbf{x}, \cdot) = N(\mathbf{x}, \sqrt{2}I_d)$ or $Q_f(x_i, dx_i) = N(x_i, \sqrt{2})$, where step-size are chosen following the guidance in Roberts et al. (1997) for univariate Metropolis steps. We plot in Figure 9 the average meeting times for coupled chains with different strategies, as the target dimension d grows. As one might expect, Figure 9 shows that the strategies

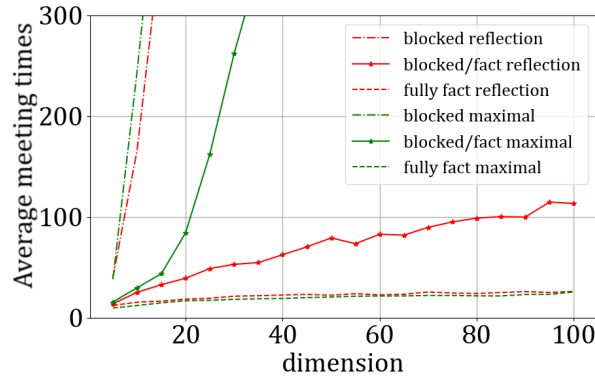


Figure 9: Average meeting times for different dimensions, Laplace target.

yielding smaller meeting times are those leveraging the independence structure of the target, proposing and accepting the components independently. *Blocked* strategies instead generally

perform worse, with the sole exception of *block/fact* reflection, due to the intrinsic contraction properties of Algorithm 6.

To better illustrate the phenomenon, Figure 10 plots the proportion of components that did not meet for the same chains as in Figure 9, for $d = \{3, 100\}$.

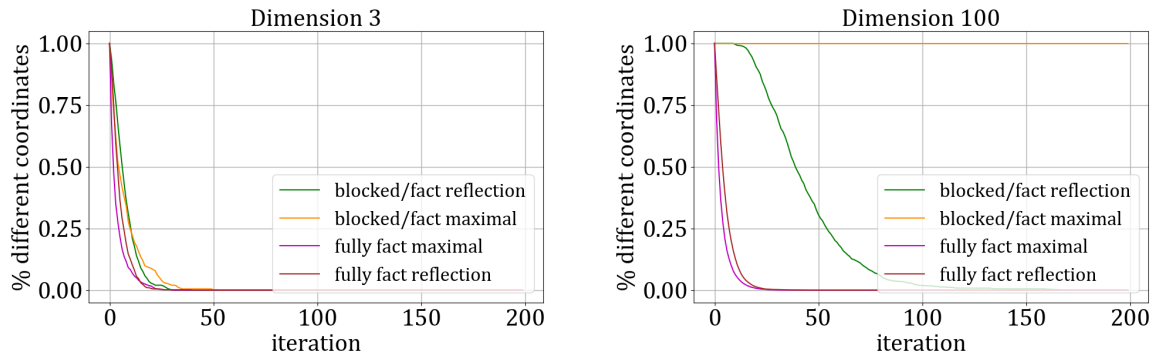


Figure 10: Estimated percentage of non coalesced components for blocked/component-wise proposals and component-wise acceptance; $d = 3, 100$.

The above examples suggest that, in case of conditionally independent blocks, fully-factorized couplings of the MH updates are preferable. This is coherent with the consideration that, in the fully-factorized case, the overall meeting time, which coincides with the one of the slowest component that coalesces, is simply the supremum of d independent random variables, hence typically growing logarithmically as the dimensionality grows (or at least sub-linearly, see [Correa and Romero \(2021\)](#)).

C Algorithmic implementation details

In this section, we report the explicit expressions for the full-conditional distributions required to implement the proposed algorithms for Models 1 and 3.

C.1 Full conditionals for Model 1

Under (1), the conditional distributions required to implement Algorithm 2 are

$$\begin{aligned} \mathcal{L}(\mu|\mathbf{a}^{(-k)}, \boldsymbol{\tau}, \mathbf{y}) &= N\left(\frac{1}{\sum_j s_j^{(k)}} \sum_j s_j^{(k)} \left(\tilde{y}_j^{(k)} - \frac{\sum_{l \neq k} \sum_i a_i^{(l)} n_{ji}^{(k,l)}}{n_j^{(k)}}\right), \frac{1}{\tau_k \sum_j s_j^{(k)}}\right), \\ \mathcal{L}(a_i^{(k)}|\mathbf{a}^{(-k)}, \mu, \boldsymbol{\tau}, \mathbf{y}) &= N\left(\frac{n_i^{(k)} \tau_0}{n_i^{(k)} \tau_0 + \tau_k} \left(\tilde{y}_i^{(k)} - \mu - \frac{\sum_{l \neq k, 0} \sum_{j=1}^{I_l} a_j^{(l)} n_{ij}^{(k,l)}}{n_i^{(k)}}\right), \frac{1}{n_i^{(k)} \tau_0 + \tau_k}\right), \\ \mathcal{L}(\tau_k|\mathbf{a}, \mu, \boldsymbol{\tau}^{-k}, \mathbf{y}) &= \text{Gamma}\left(\frac{I_k - 1}{2}, \frac{2}{\sum_{i=1}^{I_k} (a_i^{(k)})^2}\right), \end{aligned}$$

where $n_i^{(k)} = \sum_{n=1}^N \mathbb{I}(i_k[n] = i)$, $s_j^{(k)} = n_j^{(k)} \tau_0 / (\tau_k + n_j^{(k)} \tau_0)$, $n_{ji}^{(k,l)} = \sum_{n=1}^N \mathbb{I}(i_k[n] = j) \mathbb{I}(i_l[n] = i)$ denotes the number of observations of level j of factor k and i of factor l and finally $\tilde{y}_i^{(k)} = \sum_{n: i_k[n]=i} y_n / |\{n : i_k[n] = i\}|$ is the average of all observations with level i on factor k . See also

(Papaspiliopoulos et al., 2019, Eq. 4 and Prop. 2) for similar expressions.

C.2 Local centering algorithm for Model 3

Under (3), the conditional distributions required to implement Algorithm 4 are

$$\begin{aligned}\mathcal{L}(\mathbf{u}_i|\mathbf{v}, \rho, \tau_0, \mathbf{y}) &= N(\boldsymbol{\mu}_{\mathbf{u}_i}, Q_{\mathbf{u}_i}^{-1}), & \mathcal{L}(\bar{\mathbf{u}}_i|\mathbf{v}, \rho, \tau_0, \mathbf{y}) &= \frac{1}{\rho}N(\boldsymbol{\mu}_{\mathbf{u}_i}, Q_{\mathbf{u}_i}^{-1}), \\ \mathcal{L}(\mathbf{v}_j|\mathbf{u}, \rho, \tau_0, \mathbf{y}) &= N(\boldsymbol{\mu}_{\mathbf{v}_j}, Q_{\mathbf{v}_j}^{-1}), & \mathcal{L}(\bar{\mathbf{v}}_j|\mathbf{u}, \rho, \tau_0, \mathbf{y}) &= \frac{1}{\rho}N(\boldsymbol{\mu}_{\mathbf{v}_j}, Q_{\mathbf{v}_j}^{-1}),\end{aligned}$$

where $\boldsymbol{\mu}_{\mathbf{u}_i}$, $\boldsymbol{\mu}_{\mathbf{v}_j}$, $Q_{\mathbf{u}_i} = (q_{rs})_{r,s=1}^d$ and $Q_{\mathbf{v}_j} = (p_{rs})_{r,s=1}^d$ are given by

$$\begin{aligned}q_{rr} &= 1 + \tau_0\rho^2 \sum_{n:i[n]=i} v_{j[n],r}^2, & p_{rr} &= 1 + \tau_0\rho^2 \sum_{n:j[n]=j} u_{i[n],r}^2 \text{ for } r = 1, \dots, d, \\ q_{rs} &= \tau_0\rho^2 \sum_{n:i[n]=i} v_{j[n],r}v_{j[n],s}, & p_{rs} &= \tau_0\rho^2 \sum_{n:j[n]=j} u_{i[n],r}u_{i[n],s}, \text{ for } r, s = 1, \dots, d, \\ \boldsymbol{\mu}_{\mathbf{u}_i} &= Q_{\mathbf{u}_i}^{-1} \left(\tau_0\rho \sum_{n:i[n]=i} \mathbf{v}_{j[n]}y_n \right), & \boldsymbol{\mu}_{\mathbf{v}_j} &= Q_{\mathbf{v}_j}^{-1} \left(\tau_0\rho \sum_{n:j[n]=j} \mathbf{u}_{i[n]}y_n \right),\end{aligned}$$

and

$$\begin{aligned}\mathcal{L}(\rho^{-2}|\bar{\mathbf{u}}, \mathbf{v}, \tau_0, \mathbf{y}) &= \text{Gamma} \left(a + \frac{dI_1}{2}, \left(\frac{1}{b} + \sum_{i=1}^{I_1} \frac{\|\bar{\mathbf{u}}_i\|^2}{2} \right)^{-1} \right), \\ \mathcal{L}(\rho^{-2}|\mathbf{u}, \bar{\mathbf{v}}, \tau_0, \mathbf{y}) &= \text{Gamma} \left(a + \frac{dI_2}{2}, \left(\frac{1}{b} + \sum_{j=1}^{I_2} \frac{\|\bar{\mathbf{v}}_j\|^2}{2} \right)^{-1} \right), \\ \mathcal{L}(\tau_0|\mathbf{u}, \mathbf{v}, \rho, \mathbf{y}) &= \text{Gamma} \left(c + \frac{N}{2}, \left(\frac{1}{d} + \sum_{n=1}^N \frac{(y_n - \rho\mathbf{u}_{i[n]}\mathbf{v}_{j[n]})^2}{2} \right)^{-1} \right).\end{aligned}$$

For the vanilla scheme with improper prior $p(\rho) \propto 1$, then

$$\mathcal{L}(\rho^{-2}|\mathbf{u}, \mathbf{v}, \tau_0, \mathbf{y}) = TG \left(\frac{\sum_{n=1}^N \mathbf{u}_{i[n]}^\top \mathbf{v}_{j[n]} y_n}{\sum_{n=1}^N (\mathbf{u}_{i[n]}^\top \mathbf{v}_{j[n]})^2}, \frac{1}{\tau_0 \sum_{n=1}^N (\mathbf{u}_{i[n]}^\top \mathbf{v}_{j[n]})^2}; 0, +\infty \right). \quad (23)$$

We report in Algorithm 9 a more detailed pseudo-code for implementing the local centering approach described in Algorithm 4.

Algorithm 9: One iteration of BGS with local centering for Model 3

$$\begin{aligned}
& \bar{\mathbf{u}} = \rho \cdot \mathbf{u} \\
& \rho = \left(\text{Gamma} \left(a + \frac{dI_1}{2}, \left(\frac{1}{b} + \sum_{i=1}^{I_1} \frac{\|\bar{\mathbf{u}}_i\|^2}{2} \right)^{-1} \right) \right)^{-\frac{1}{2}} \\
& \text{for } i = 1, \dots, I_1 \text{ do} \\
& \quad \bar{\mathbf{u}}_i \sim N(\boldsymbol{\mu}_{\bar{\mathbf{u}}_i}, Q_{\bar{\mathbf{u}}_i}^{-1}) \\
& \mathbf{u} = \bar{\mathbf{u}}/\rho \\
& \bar{\mathbf{v}} = \rho \cdot \mathbf{v} \\
& \rho = \left(\text{Gamma} \left(a + \frac{dI_2}{2}, \left(\frac{1}{b} + \sum_{i=1}^{I_2} \frac{\|\bar{\mathbf{v}}_i\|^2}{2} \right)^{-1} \right) \right)^{-\frac{1}{2}} \\
& \text{for } i = 1, \dots, I_2 \text{ do} \\
& \quad \bar{\mathbf{v}}_i \sim N(\boldsymbol{\mu}_{\bar{\mathbf{v}}_i}, Q_{\bar{\mathbf{v}}_i}^{-1}) \\
& \mathbf{v} = \bar{\mathbf{v}}/\rho \\
& \tau_0 \sim \text{Gamma} \left(c + \frac{N}{2}, \left(\frac{1}{d} + \sum_{n=1}^N \frac{(y_n - \rho \mathbf{u}_{i[n]} \mathbf{v}_{j[n]})^2}{2} \right)^{-1} \right)
\end{aligned}$$

D Proofs

D.1 Proofs of the results in Section 4.1

D.1.1 Proof of Theorem 1

The proof of Theorem 1 builds upon Lemma 7 and Lemma 8, whose statements and proofs are deferred after the end of the former.

Proof of Theorem 1. In the following, we will state the results assuming that $\mathbf{X}^0, \mathbf{Y}^0$ are fixed, or equivalently conditioning on their values, omitting the explicit conditioning in the notation for brevity.

Define $(\mathcal{D}^t)_{t \geq 0}$ as

$$\mathcal{D}^t := \|\mathcal{L}(\mathbf{X}^{t+1}|\mathbf{X}^t) - \mathcal{L}(\mathbf{Y}^{t+1}|\mathbf{Y}^t)\|_{TV} \quad t \geq 0, \quad (24)$$

Denote by $(t_k)_{k \geq 1}$ as the sequence of times at which $\mathcal{D}^t < \varepsilon$, i.e.

$$t_k := \min\{t > t_{k-1} : \mathcal{D}^t < \varepsilon\} \quad k \geq 1, \quad (25)$$

with $t_0 := -1$ by convention. Note that by the form of Algorithm 1, the t_k 's are exactly the iterations at which a maximal coupling is implemented. Also, let A_k be a binary variable indicating whether the maximal coupling attempt at t_k is successful, i.e.

$$A_k := \begin{cases} 1 & \text{if } \mathbf{X}^{t_k+1} = \mathbf{Y}^{t_k+1} \\ 0 & \text{otherwise} \end{cases} \quad k \geq 1. \quad (26)$$

By faithfulness, $A_k = 1$ implies that $\mathbf{X}^t = \mathbf{Y}^t$, for all $t \geq t_k$ and by convention $A_{k'} = 1$ for all $k' > k$. Note also that from (25) and (26), one has

$$\mathbb{E}[1 - A_k | \mathbf{X}^{t_k}, \mathbf{Y}^{t_k}, A_{k-1} = 0] = \Pr(A_k = 0 | \mathbf{X}^{t_k}, \mathbf{Y}^{t_k}, A_{k-1} = 0) = \mathcal{D}^{t_k}. \quad (27)$$

Thus, T can be written as

$$T = t_1 + 1 + \sum_{k=1}^{+\infty} (1 - A_k)(t_{k+1} - t_k). \quad (28)$$

We bound $\mathbb{E}[T]$ using the form of (28). In particular, by Lemma 7, we have

$$t_1 + 1 \leq f_1(\|L^{-1}(\mathbf{X}^0 - \mathbf{Y}^0)\|, \varepsilon, B), \quad (29)$$

for f_1 defined therein. Note that, conditionally on $(\mathbf{X}^0, \mathbf{Y}^0)$, the bound is deterministic: provided the chains evolve via *crn* coupling from iteration 1 up to t_1 , \mathcal{D}^{t_1} is a deterministic function of the starting points $(\mathbf{X}^0, \mathbf{Y}^0)$ and matrices B, N, L (see (34) and (35) for further details).

Considering the third addend in (28), by the definitions of \mathcal{D}^t , $(t_k)_{k \geq 1}$, $(A_k)_{k \geq 1}$ and the form of Algorithm 1, it follows that $\{A_k = 0\}$ implies $\{A_i = 0\}$ for $i \leq k$, then, exploiting the equality in (27), we get

$$\begin{aligned} \Pr(A_k = 0 | \mathbf{X}^{t_k}, \mathbf{Y}^{t_k}) &= \Pr(A_1 = 0, \dots, A_{k-1} = 0, A_k = 0 | \mathbf{X}^{t_k}, \mathbf{Y}^{t_k}) \\ &= \Pr(A_1 = 0, \dots, A_{k-1} = 0 | \mathbf{X}^{t_k}, \mathbf{Y}^{t_k}) \Pr(A_k = 0 | \mathbf{X}^{t_k}, \mathbf{Y}^{t_k}, A_{k-1} = 0) \\ &\leq \varepsilon^{k-1} \mathcal{D}^{t_k} \end{aligned} \quad k \geq 1, \quad (30)$$

where the last inequality follows from the fact that $\Pr(A_j = 0 | \mathbf{X}^{t_k}, \mathbf{Y}^{t_k}) \leq \varepsilon$ for all $j = 1, \dots, k$ given that, by the form of Algorithm 1, coalescence is attempted only if it has probability greater than ε . Combining the last equality with the Monotone Convergence Theorem and Lemma 7 we can rewrite the third term of (28) as

$$\begin{aligned} \mathbb{E} \left[\sum_{k=1}^{+\infty} (1 - A_k)(t_{k+1} - t_k) \right] &= \sum_{k=1}^{+\infty} \mathbb{E} \left[\mathbb{E}[(1 - A_k)(t_{k+1} - t_k) | \mathbf{X}^{t_k}, \mathbf{Y}^{t_k}] \right] \\ &= \sum_{k=1}^{+\infty} \mathbb{E} \left[\Pr(A_k = 0 | \mathbf{X}^{t_k}, \mathbf{Y}^{t_k}) \mathbb{E}[(t_{k+1} - t_k) | \mathbf{X}^{t_k}, \mathbf{Y}^{t_k}, A_k = 0] \right] \\ &\leq \sum_{k=1}^{+\infty} \varepsilon^{k-1} \mathbb{E} \left[\mathcal{D}^{t_k} \mathbb{E}[(t_{k+1} - t_k) | \mathbf{X}^{t_k}, \mathbf{Y}^{t_k}, A_k = 0] \right]. \end{aligned} \quad (31)$$

By Lemma 8, we have

$$\mathcal{D}^{t_k} \mathbb{E}[t_{k+1} - t_k | A_k = 0, \mathbf{X}^{t_k}, \mathbf{Y}^{t_k}] \leq f_2(\varepsilon, B),$$

for f_2 defined therein. Note that the inequality above holds almost surely, i.e. with probability one. Crucially, the bound does not depend on the exact distance between the chains at time t_k , but only on ε . Substituting in (31) we obtain

$$\mathbb{E} \left[\sum_{k=1}^{+\infty} (1 - A_k)(t_{k+1} - t_k) \right] \leq f_2(\varepsilon, B) \sum_{k=1}^{+\infty} \varepsilon^{k-1} = f_2(\varepsilon, B) (1 - \varepsilon)^{-1}.$$

It then follows

$$\mathbb{E}[T] \leq 1 + f_1(\|L^{-1}(\mathbf{X}^0 - \mathbf{Y}^0)\|, \varepsilon, B) + (1 - \varepsilon)^{-1} f_2(\varepsilon, B).$$

After explicit computations

$$\begin{aligned} \mathbb{E}[T] &\leq 2 + \frac{1}{-\ln(\rho(B))} \left(\ln(\|L^{-1}(\mathbf{X}^0 - \mathbf{Y}^0)\|) - \frac{1}{2} \ln(1 - \lambda_{\min}^2(B)) - \ln(2\sqrt{2}\operatorname{erf}^{-1}(\varepsilon)) \right) \\ &+ \frac{1}{1 - \varepsilon} \cdot \left(1 + \ln(12 + 8\sqrt{2/\pi})\operatorname{erf}^{-1}(\varepsilon)/\sqrt{\pi} + \sqrt{2}(\sqrt{\pi}e)^{-1} \right). \end{aligned}$$

It is possible to further simplify the bound provided $\varepsilon < 0.5$, thus getting the expression in Theorem 1, where we set $C_0 := \ln(\|L^{-1}(\mathbf{X}^0 - \mathbf{Y}^0)\|)$ and

$$C_\varepsilon := -\ln(\operatorname{erf}^{-1}(\varepsilon)2\sqrt{2}) + 2\ln(12 + 8\sqrt{2/\pi})\operatorname{erf}^{-1}(\varepsilon) + \sqrt{2}(\sqrt{\pi}e)^{-1} \leq -\ln(\operatorname{erf}^{-1}(\varepsilon)) + 6\operatorname{erf}^{-1}(\varepsilon).$$

□

Lemma 7. *Under the assumptions of Theorem 1 we have*

$$t_1 + 1 \leq f_1(\|L^{-1}(\mathbf{X}^0 - \mathbf{Y}^0)\|, \varepsilon, B),$$

with

$$f_1(r, \varepsilon, B) = \left\lceil \frac{\ln(r) - \frac{1}{2} \ln(1 - \lambda_{\min}^2(B)) - \ln(\operatorname{erf}^{-1}(\varepsilon)2\sqrt{2})}{-\ln(\rho(B))} \right\rceil \quad r \in (0, \infty), \varepsilon \in (0, 1).$$

Proof of Lemma 7. Recall that given $p = N(\boldsymbol{\mu}, \Sigma)$ and $q = N(\boldsymbol{\nu}, \Sigma)$, it holds

$$\|p - q\|_{TV} = \operatorname{erf} \left(\sqrt{\frac{(\boldsymbol{\mu} - \boldsymbol{\nu})^\top \Sigma^{-1} (\boldsymbol{\mu} - \boldsymbol{\nu})}{8}} \right). \quad (32)$$

From (32) above, the autoregressive form of Gaussian chain in (7) and the equation of the *crn* coupling in (20), for all $t < t_1$ we have

$$\mathcal{D}^t = \operatorname{erf} \left(\sqrt{\frac{(\mathbf{X}^t - \mathbf{Y}^t)^\top B^\top (\Sigma - B\Sigma B^\top)^{-1} B (\mathbf{X}^t - \mathbf{Y}^t)}{8}} \right). \quad (33)$$

We are interested in sufficient conditions for having $\mathcal{D}_t \leq \varepsilon$. Set $N := L^{-1}BL$, with $LL^\top = \Sigma$, and also

$$\begin{aligned} \mathbf{d}^t &:= L^{-1}B(\mathbf{X}^t - \mathbf{Y}^t) = L^{-1}B^{t+1}(\mathbf{X}^0 - \mathbf{Y}^0) \\ &= L^{-1}B^{t+1}LL^{-1}(\mathbf{X}^0 - \mathbf{Y}^0) = N^{t+1}L^{-1}(\mathbf{X}^0 - \mathbf{Y}^0), \end{aligned} \quad (34)$$

where the first equality follows since the draws are paired via *crn* coupling up to iteration t (see Algorithmic specification 1). Then (33) becomes

$$\mathcal{D}^t = \operatorname{erf} \left(\sqrt{\frac{(\mathbf{d}^t)^\top (1_d - NN^\top)^{-1} \mathbf{d}^t}{8}} \right), \quad (35)$$

where we used $(\Sigma - B\Sigma B^\top)^{-1} = (LL^\top - BLL^\top B^\top)^{-1} = L^{-\top}(1 - NN^\top)^{-1}L^{-1}$. Given π reversibility of P , one has $\Sigma B^\top = B\Sigma$ (Khare and Zhou, 2009, Proposition 4.27), implying

$N = N^\top$. Hence by properties of the spectral radius and symmetric matrices

$$\begin{aligned}
(\mathbf{d}^t)^\top (1 - NN^\top)^{-1} \mathbf{d}^t &\leq \|\mathbf{d}^t\|^2 \rho(1_d - NN^\top)^{-1} \\
&= \|N^{t+1} L^{-1}(\mathbf{X}^0 - \mathbf{Y}^0)\|^2 \rho(1_d - NN^\top)^{-1} \\
&\leq \|L^{-1}(\mathbf{X}^0 - \mathbf{Y}^0)\|^2 \frac{\|N^{t+1}\|_2^2}{\rho(1_d - NN^\top)} \\
&\leq \|L^{-1}(\mathbf{X}^0 - \mathbf{Y}^0)\|^2 \frac{\rho(N)^{2(t+1)}}{1 - \lambda_{\min}(NN^\top)},
\end{aligned} \tag{36}$$

where for $A \in \mathbb{R}^{m,n}$ we denote by $\|A\|_2 = \sup_{\mathbf{x} \neq 0, \mathbf{x} \in \mathbb{R}^n} \frac{\|A\mathbf{x}\|_2}{\|\mathbf{x}\|_2}$ the induced 2 norm. Combining (35) and (36), a sufficient condition for $\mathcal{D}_t \leq \varepsilon$ is to have

$$\|L^{-1}(\mathbf{X}^0 - \mathbf{Y}^0)\|^2 \frac{\rho(N)^{2(t+1)}}{1 - \lambda_{\min}(NN^\top)} < 8 (\operatorname{erf}^{-1}(\varepsilon))^2. \tag{37}$$

Note that this also implies that

$$\|\mathbf{d}^t\|^2 \leq 8 (\operatorname{erf}^{-1}(\varepsilon))^2 \left(1 - \lambda_{\min}(NN^\top)\right). \tag{38}$$

Again by π -reversibility of P , since $N = N^\top$, one has $\lambda_{\min}(NN^\top) = \lambda_{\min}(N)^2 = \lambda_{\min}(B)^2$ and also $\rho(B) = \rho(N)$. Substituting into (37) and solving for t we get the result. \square

Lemma 8. *Under the assumptions of Theorem 1 we have*

$$\mathcal{D}^{t_k} \mathbb{E}[t_{k+1} - t_k | A_k = 0, \mathbf{X}^{t_k}, \mathbf{Y}^{t_k}] \leq f_2(\varepsilon, B) \quad a.s.,$$

where

$$f_2(\varepsilon, B) = \left\lceil \frac{\ln(12 + 8\sqrt{2/\pi}) \operatorname{erf}^{-1}(\varepsilon) / \sqrt{\pi} + 2\sqrt{2}(\sqrt{\pi}e)^{-1}}{-\ln(\rho(B))} \right\rceil.$$

Proof of Lemma 8. The proof of Lemma 8 relies on two different parts. In the first we bound the expected square distance between \mathbf{X}^{t_k+1} and \mathbf{Y}^{t_k+1} conditionally on $A_k = 0$, and this is achieved controlling the first and second moments of truncated Gaussians (see Lemma 2 in the main body of the paper). Then we bound the product of the former (possibly growing to $+\infty$ as ε goes to zero) times the total variation distance between the chains themselves.

We start by noting that the result of Lemma 7 can be extended for every $t_k - t_{k-1}$ with $k \geq 2$, since the arguments rely only on the form of Algorithm 1 and on the expression in (32). It follows that

$$\mathbb{E}[t_{k+1} - t_k | A_k = 0, \mathbf{X}^{t_k}, \mathbf{Y}^{t_k}] \leq \mathbb{E}[f_1(\|L^{-1}(\mathbf{X}^{t_k+1} - \mathbf{Y}^{t_k+1})\|, \varepsilon, B) | A_k = 0, \mathbf{X}^{t_k}, \mathbf{Y}^{t_k}].$$

Thus one can write

$$\begin{aligned}
\mathcal{D}^{t_k} \mathbb{E}[t_{k+1} - t_k | A_k = 0, \mathbf{X}^{t_k}, \mathbf{Y}^{t_k}] &\leq \mathcal{D}^{t_k} \mathbb{E}[f_1(\|L^{-1}(\mathbf{X}^{t_k+1} - \mathbf{Y}^{t_k+1})\|, \varepsilon, B) | A_k = 0, \mathbf{X}^{t_k}, \mathbf{Y}^{t_k}] \\
&\leq \mathcal{D}^{t_k} f_1(\mathbb{E}[\|L^{-1}(\mathbf{X}^{t_k+1} - \mathbf{Y}^{t_k+1})\| | A_k = 0, \mathbf{X}^{t_k}, \mathbf{Y}^{t_k}], \varepsilon, B),
\end{aligned} \tag{39}$$

where the last inequality follows from Jensen applied to $f_1(\cdot, \varepsilon, B)$, and in particular to the

logarithmic function in its expression. Define $z^{t_k} := \sqrt{(\mathbf{d}^{t_k})^\top (1 - NN^\top)^{-1} \mathbf{d}^{t_k}}$, with \mathbf{d}^t as in (34). Since at iteration t_k we implement maximal reflection coupling, we can apply Lemma 2 on the argument of f_1 , provided that $z_{t_k} \leq 1$, thus getting

$$\mathbb{E} [\|L^{-1}(\mathbf{X}^{t_k+1} - \mathbf{Y}^{t_k+1})\|^2 | A_k = 0] \leq \frac{\|L^{-1}B(\mathbf{X}^{t_k} - \mathbf{Y}^{t_k})\|^2}{(z^{t_k})^4} \left(12 + 8\sqrt{\frac{2}{\pi}}\right).$$

Hence substituting the bound in the expression of f_1 in (39), one gets

$$\begin{aligned} & \mathcal{D}^{t_k} \mathbb{E}[(t_{k+1} - t_k) | A_k = 0, \mathbf{X}^{t_k}, \mathbf{Y}^{t_k}] \\ & \leq \frac{\mathcal{D}^{t_k}}{-\ln(\rho(B))} \left(\frac{1}{2} \ln(\|\mathbf{d}^{t_k}\|^2) - \frac{1}{2} \ln(1 - \lambda_{\min}^2(B)) - \ln(2\sqrt{2} \operatorname{erf}^{-1}(\varepsilon)) \right) \end{aligned} \quad (40)$$

$$\leq \frac{\mathcal{D}^{t_k}}{-2 \ln(\rho(B))} \left(-2 \ln(z_{t_k}) + \ln(12 + 8\sqrt{2/\pi}) \right) \quad (41)$$

$$\leq \frac{z^{t_k}}{-\sqrt{2\pi} \ln(\rho(B))} \left(-4 \ln(z_{t_k}) + \ln(12 + 8\sqrt{2/\pi}) \right) \quad (42)$$

$$\leq \frac{\ln(12 + 8\sqrt{2/\pi}) \operatorname{erf}^{-1}(\varepsilon) / \sqrt{\pi} + \sqrt{2}(\sqrt{\pi}e)^{-1}}{-\ln(\rho(B))}, \quad (43)$$

where from (40) to (41) we used the condition in (38) and subsequent simplifications, and from (41) to (42) we instead used that, by construction and (33), one has $\mathcal{D}^{t_k} = \operatorname{erf}(z^{t_k}/\sqrt{8})$. Finally it holds $\operatorname{erf}(x) < \frac{2}{\sqrt{\pi}}x$ and $-\ln(x)x \leq 1/e$ for $x > 0$, and so $z^{t_k} \leq 2\sqrt{2} \operatorname{erf}^{-1}(\varepsilon)$ by (34). \square

D.1.2 Proof of Lemma 2

In order to prove Lemma 2, we use an instrumental lemma, namely Lemma 9. In the following, we denote $TG(\mu, \sigma^2; a, b)$ a truncated Gaussian with mean parameter μ , variance parameter σ^2 , and constrained between a and b .

Lemma 9. *Let $\sigma \in (0, \infty)$ and $\alpha \in \mathbb{R}$ and $X \sim TG(0, \sigma^2; \alpha, +\infty)$. It holds that*

$$\mathbb{E}[X] \leq \max(0, \alpha) + \sigma \sqrt{\frac{2}{\pi}}, \quad \mathbb{E}[X^2] \leq \sigma^2 + \alpha^2 + \sqrt{\frac{2}{\pi}} \alpha \sigma.$$

Proof of Lemma 9. For $T \sim TG(\mu, \sigma^2; \alpha, +\infty)$, we know

$$\mathbb{E}[T] = \mu + \frac{\phi\left(\frac{\alpha-\mu}{\sigma}\right)}{1 - \Phi\left(\frac{\alpha-\mu}{\sigma}\right)} \sigma, \quad (44)$$

$$\mathbb{E}[T^2] = \sigma^2 + \sigma^2 \frac{\frac{\alpha-\mu}{\sigma} \phi\left(\frac{\alpha-\mu}{\sigma}\right)}{1 - \Phi\left(\frac{\alpha-\mu}{\sigma}\right)} + \mu^2 + 2\mu\sigma \frac{\phi\left(\frac{\alpha-\mu}{\sigma}\right)}{1 - \Phi\left(\frac{\alpha-\mu}{\sigma}\right)}, \quad (45)$$

where $\phi(\cdot), \Phi(\cdot)$ denote respectively the density and the cumulative functions of the standard normal distribution. We divide the proof in the cases $\alpha < 0$ and $\alpha \geq 0$.

Consider $\alpha < 0$. Denote by $c_{\mu, \sigma^2; \alpha}$ the normalizing constant $c_{\mu, \sigma^2; \alpha} = \int_{\alpha}^{+\infty} e^{-\frac{(x-\mu)^2}{2\sigma^2}} dx$. Since

$X \sim TG(0, \sigma^2; \alpha, +\infty)$ and $\alpha < 0$, we have

$$\mathbb{E}[X] = \int_{\alpha}^{+\infty} x \frac{e^{-\frac{x^2}{2\sigma^2}}}{c_{0,\sigma^2;\alpha}} dx \leq \int_0^{+\infty} x \frac{e^{-\frac{x^2}{2\sigma^2}}}{c_{0,\sigma^2;\alpha}} dx.$$

Multiplying and dividing by $c_{0,\sigma^2;0}$ and recalling that for $Y \sim TG(0, \sigma^2; 0, +\infty)$ one has $\mathbb{E}[Y] = \sqrt{\frac{2}{\pi}}\sigma$ from (44), then

$$\int_0^{+\infty} x \frac{e^{-\frac{x^2}{2\sigma^2}}}{c_{0,\sigma^2;\alpha}} dx \leq \frac{c_{0,\sigma^2;0}}{c_{0,\sigma^2;\alpha}} \sqrt{\frac{2}{\pi}}\sigma.$$

Furthermore since $\frac{c_{0,\sigma^2;0}}{c_{0,\sigma^2;\alpha}} = \frac{c_{0,\sigma^2;0}}{\int_{\alpha}^0 e^{-\frac{t^2}{2\sigma^2}} dx + c_{0,\sigma^2;0}} < 1$, it follows that

$$\mathbb{E}[X] \leq \sqrt{\frac{2}{\pi}}\sigma. \quad (46)$$

Consider now $\alpha \geq 0$. We prove

$$\mathbb{E}[X] \leq \alpha + \sqrt{\frac{2}{\pi}}\sigma = \mathbb{E}[Y], \quad (47)$$

with $Y \sim TG(\alpha, \sigma^2; \alpha, +\infty)$. We exploit stochastic ordering: if there exists a coupling between $X \sim TG(0, \sigma^2; \alpha, +\infty)$ and $Y \sim TG(\alpha, \sigma^2; \alpha, +\infty)$ such that $\Pr(X < Y) = 1$, then the desired result follows. Given that the Gaussian distribution belongs to the exponential family, it has monotone likelihood ratio in its canonical statistics, that is x , hence implying stochastic ordering.

For the second moment, by (45) and the bound just found in (46) and (47), we get

$$\mathbb{E}[X^2] = \sigma^2 + \alpha\sigma\mathbb{E}[Y] \leq \sigma^2 + \alpha^2 + \sqrt{\frac{2}{\pi}}\alpha\sigma,$$

for $Y \sim TG(0, 1; \frac{\alpha}{\sigma}, +\infty)$. □

Proof of Lemma 2. We first prove the bound for $d = 1$ and then generalize. The explicit form of Algorithm 6 will be exploited repeatedly throughout the proof.

Suppose $X \sim N(\xi, \sigma^2)$, $Y \sim N(\nu, \sigma^2)$ where, without loss of generality, $\xi > \nu$, and define $z := \frac{\xi - \nu}{\sigma} > 0$, $W \sim U(0, 1)$, $\dot{X} \sim N(0, 1)$ as in Algorithm 1. Coalescence is not reached only whenever $W > \frac{s(\dot{X} + z)}{s(\dot{X})}$, or equivalently

$$\dot{X} > -\frac{z}{2} - \frac{\ln(W)}{z}.$$

Then it holds $\dot{X}|W, X \neq Y \sim TN\left(0, 1; -\frac{z}{2} - \frac{\ln(W)}{z}, +\infty\right)$. Furthermore, whenever coalescence is not reached we have $X = \sigma\dot{X} + \mu$ and $Y = -\sigma\dot{X} + \nu$, then, for $a > 0$

$$\begin{aligned} \mathbb{E}[a^2(X - Y)^2|W, X \neq Y] &= a^2\mathbb{E}[(2\sigma\dot{X} + \xi - \nu)^2|W, X \neq Y] \\ &= a^2\sigma^2\mathbb{E}[(2\dot{X} + z)^2|W, X \neq Y] \\ &= a^2\sigma^2 \left[4\mathbb{E}[\dot{X}^2|W, X \neq Y] + z^2 + 4z\mathbb{E}[\dot{X}|W, X \neq Y] \right]. \end{aligned}$$

Therefore, one can apply the bounds of Lemma 9 to get bounds for the squared distance among the two distributions.

We now extend for the multivariate case, leading to the result. Again denote by $\mathbf{z} := \Sigma^{-\frac{1}{2}}(\boldsymbol{\xi} - \boldsymbol{\nu})$, $\dot{\mathbf{X}} \sim N_d(\mathbf{0}, 1_d)$, $W \sim U(0, 1)$ and $\mathbf{e} := \frac{\mathbf{z}}{\|\mathbf{z}\|}$ as in the formulation of Algorithm 6. Whenever coupling is not reached it holds that

$$\mathbf{z}^\top \dot{\mathbf{X}} \geq -\frac{\|\mathbf{z}\|^2}{2} - \ln(W).$$

It is possible to find an orthonormal matrix R , i.e. a rotation matrix, such that the first coordinate of $\hat{\mathbf{X}} := R\dot{\mathbf{X}}$ becomes \mathbf{z} and has squared norm exactly $\mathbf{z}^\top \dot{\mathbf{X}}$. It then follows from orthonormality and symmetry of $\dot{\mathbf{X}}$ that $\hat{\mathbf{X}} \sim N_d(\mathbf{0}, 1_d)$. Whenever coupling is not reached, only the first coordinate $\hat{X}_1 = \mathbf{z}^\top \dot{\mathbf{X}}$ is constrained to be greater or equal than $-\frac{\|\mathbf{z}\|^2}{2} - \ln(W)$, independently on the other coordinates, i.e. $\mathbf{z}^\top \dot{\mathbf{X}} | \mathbf{X} \neq \mathbf{Y}, W \sim TN(0, 1; -\frac{\|\mathbf{z}\|^2}{2} - \ln(W))$. For this coordinate, the bounds in Lemma 9 still hold, giving

$$\mathbb{E}[\mathbf{z}^\top \dot{\mathbf{X}} | \mathbf{X} \neq \mathbf{Y}, W] \leq \max\left(0, -\frac{\|\mathbf{z}\|^2}{2} - \ln(W)\right) + \sqrt{\frac{2}{\pi}}, \quad (48)$$

$$\mathbb{E}[(\mathbf{z}^\top \dot{\mathbf{X}})^2 | \mathbf{X} \neq \mathbf{Y}, W] \leq 1 + \left(-\frac{\|\mathbf{z}\|^2}{2} - \ln(W)\right)^2 + \sqrt{\frac{2}{\pi}} \left(-\frac{\|\mathbf{z}\|^2}{2} - \ln(W)\right). \quad (49)$$

Then, leveraging the expression of $\mathbf{X} - \mathbf{Y} | \mathbf{X} \neq \mathbf{Y}$ and \mathbf{e} , we get

$$\begin{aligned} \mathbb{E}[\|A(\mathbf{X} - \mathbf{Y})\|^2 | \mathbf{X} \neq \mathbf{Y}, W] &= \mathbb{E}\left[\|A(\boldsymbol{\xi} - \boldsymbol{\nu} + 2(\mathbf{e}^\top \dot{\mathbf{X}})\Sigma^{\frac{1}{2}}\mathbf{e})\|^2 | \mathbf{X} \neq \mathbf{Y}, W\right] \\ &= \mathbb{E}\left[\left\|A(\boldsymbol{\xi} - \boldsymbol{\nu})\left(1 + \frac{2}{\|\mathbf{z}\|^2}(\mathbf{z}^\top \dot{\mathbf{X}})\right)\right\|^2 | \mathbf{X} \neq \mathbf{Y}, W\right] \\ &= \|A(\boldsymbol{\xi} - \boldsymbol{\nu})\|^2 \mathbb{E}\left[1 + \frac{4}{\|\mathbf{z}\|^4}(\mathbf{z}^\top \dot{\mathbf{X}})^2 + \frac{4}{\|\mathbf{z}\|^2}\mathbf{z}^\top \dot{\mathbf{X}} | \mathbf{X} \neq \mathbf{Y}, W\right] \\ &\leq \|A(\boldsymbol{\xi} - \boldsymbol{\nu})\|^2 \left[2 + \frac{4}{\|\mathbf{z}\|^4}\left(1 + \ln^2(W) - \sqrt{\frac{2}{\pi}}\ln(W)\right) + \frac{4}{\|\mathbf{z}\|^2}\left(\ln(W) + 1/\sqrt{2\pi}\right)\right. \\ &\quad \left.+ \max\left(0, -2 - \frac{4}{\|\mathbf{z}\|^2}\ln(W)\right)\right]. \end{aligned} \quad (50)$$

By law of iterated expectations, one has

$$\mathbb{E}[\|A(\mathbf{X} - \mathbf{Y})\|^2 | \mathbf{X} \neq \mathbf{Y}] = \mathbb{E}\left[\mathbb{E}[\|A(\mathbf{X} - \mathbf{Y})\|^2 | \mathbf{X} \neq \mathbf{Y}, W]\right]. \quad (51)$$

Hence we compute

$$\begin{aligned} \mathbb{E}\left[\max\left(0, -2 - \frac{4}{\|\mathbf{z}\|^2}\ln(W)\right)\right] &= \int_0^1 \max\left(0, -2 - \frac{4}{\|\mathbf{z}\|^2}\ln(w)\right) dw \\ &= \frac{4}{\|\mathbf{z}\|^2} \int_0^{e^{-\frac{\|\mathbf{z}\|^2}{2}}} \left(-\frac{\|\mathbf{z}\|^2}{2} - \ln(w)\right) dw = \frac{4}{\|\mathbf{z}\|^2} e^{-\frac{\|\mathbf{z}\|^2}{2}}. \end{aligned}$$

Knowing $\mathbb{E}[\ln(W)] = -1$, $\mathbb{E}[\ln^2(W)] = 2$, plugging (50) in (51), one gets

$$\begin{aligned} \mathbb{E}[\|A(\mathbf{X} - \mathbf{Y})\|^2 | \mathbf{X} \neq \mathbf{Y}] &= \mathbb{E}_W [\mathbb{E}[\|A(\mathbf{X} - \mathbf{Y})\|^2 | \mathbf{X} \neq \mathbf{Y}, W]] \\ &\leq \|A(\boldsymbol{\xi} - \boldsymbol{\nu})\|^2 \left(2 + \frac{4}{\|\mathbf{z}\|^4} (3 + \sqrt{2/\pi}) + \frac{4}{\|\mathbf{z}\|^2} (e^{-\frac{\|\mathbf{z}\|^2}{2}} - 1 + 1/\sqrt{2\pi}) \right). \end{aligned}$$

Given that $\|\mathbf{z}\| \leq 1$ by hypothesis, then

$$\mathbb{E}[\|A(\mathbf{X} - \mathbf{Y})\|^2 | \mathbf{X} \neq \mathbf{Y}] \leq \|A(\boldsymbol{\xi} - \boldsymbol{\nu})\|^2 \left(\frac{12 + 8\sqrt{\frac{2}{\pi}}}{\|\mathbf{z}\|^4} \right).$$

□

D.1.3 Proof of the claim in Remark 1

Let $\mathbf{x} \sim \pi = N(\boldsymbol{\mu}, \Sigma)$ divided in K blocks as in Section 3.4. Consider $D \in \mathbb{R}^{d \times d}$ block-diagonal matrix with same blocking structure and denote by $\mathbf{x}_D := D\mathbf{x}$ and by π_D the transformed random variable and the induced distribution respectively. We now show that both the distribution of the meeting time induced by Algorithm 1 and the bound in (9) will not change.

From well known Gaussian properties, it follows $\pi_D = N(D\boldsymbol{\mu}, D\Sigma D^\top)$, furthermore simple calculations point that $B_D = DBD^{-1}$ and $L_D = DL$. Let $(\mathbf{X}^t, \mathbf{Y}^t)_{t \geq 1}$ as in Theorem 1 and $(\mathbf{X}_D^t, \mathbf{Y}_D^t)_{t \geq 1}$ the chain targeting π_D starting at $(\mathbf{X}_D^0, \mathbf{Y}_D^0) := (D\mathbf{X}^0, D\mathbf{Y}^0)$. It follows that $\|\mathcal{L}(\mathbf{X}^{t+1} | \mathbf{X}^t) - \mathcal{L}(\mathbf{Y}^{t+1} | \mathbf{Y}^t)\|_{TV} = \|\mathcal{L}(\mathbf{X}_D^{t+1} | \mathbf{X}_D^t) - \mathcal{L}(\mathbf{Y}_D^{t+1} | \mathbf{Y}_D^t)\|_{TV}$ for all $t \geq 1$, hence the equal behaviour of Algorithm 1.

D.2 Proofs of Theorem 2

The proof of Theorem 2 builds upon two results presented in Lemma 10 and Lemma 11 below. In this section, under the assumption of Theorem 2, we will always assume $P^{(F)} = P_2 P_1$ and $B^{(F)}$ as in Lemma 1 accordingly. Let also L be the block triangular matrix such that $LL^\top = \Sigma$.

Lemma 10. *Under the assumption of Theorem 2, for $N^{(F)} := L^{-1}B^{(F)}L$, it holds*

$$\lambda_{\min} \left(N^{(F)} (N^{(F)})^\top \right) = 0.$$

Proof of Lemma 10. Leveraging the results in Remark 1, we find a suitable block diagonal linear transformation D of the chain and compute for the transformed chain $\lambda_{\min}(N_D^{(F)}(N_D^{(F)})^\top)$ (using the same notation as in Remark 1), then, since $N_D^{(F)} = L_D^{-1}B_D^{(F)}L_D = L^{-1}D^{-1}DB^{(F)}D^{-1}DL = L^{-1}B^{(F)}L = N^{(F)}$, we get the result. Consider $D = \text{diag}(Q_{(1,1)}, Q_{(2,2)})^{\frac{1}{2}}$. It follows that the precision matrix of π_D is

$$Q_D = \left(\begin{array}{c|c} 1 & M \\ \hline M^\top & 1 \end{array} \right), \quad (52)$$

where $M = Q_{(1,1)}^{-\frac{1}{2}} Q_{(1,2)} Q_{(2,2)}^{-\frac{1}{2}}$. By Lemma 1, one gets

$$B_D^{(F)} = \left(\begin{array}{c|c} 0 & -M \\ \hline 0 & M^\top M \end{array} \right).$$

If $L_D L_D^\top = \Sigma_D$ (with Σ_D full rank), then it follows $L_D^{-\top} L_D^{-1} = Q_D$. Suppose now

$$L_D^{-1} = \left(\begin{array}{c|c} A & 0 \\ \hline B & C \end{array} \right), \quad (53)$$

for A, B, C matrices of suitable dimensions, one has

$$\begin{cases} A^\top A + B^\top B = 1 \\ B^\top C = M \\ C^\top C = 1. \end{cases} \quad (54)$$

And therefore, solving for $N_D^{(F)}$

$$N_D^{(F)} = \left(\begin{array}{c|c} 1 - AA^\top & -AB^\top \\ \hline 0 & 0 \end{array} \right).$$

From which $\lambda_{\min} \left(N_D^{(F)} (N_D^{(F)})^\top \right) = \lambda_{\min} (N N^\top) = 0$. \square

Lemma 11. *Let $B^{(F)}$ and $B^{(FB)}$ be respectively the auto-regressive matrices induced by $P^{(F)}$ of (5) and $P^{(FB)}$ of (8) for $\pi = N(\boldsymbol{\mu}, \Sigma)$, with $K = 2$ blocks. Let $N^{(F)} = L^{-1} B^{(F)} L$ and $N^{(FB)} = L^{-1} B^{(FB)} L$. For all $t > 1$ one has*

$$(B^{(F)})^t = A_2 (B^{(FB)})^{t-1},$$

with A_2 as in (57). If furthermore

$$Q = \left(\begin{array}{c|c} 1 & M \\ \hline M^\top & 1 \end{array} \right), \quad (55)$$

it holds

$$\| (N^{(F)})^t \|_2 \leq \rho \left((B^{(FB)})^{t-1} \right) = \rho \left((B^{(F)})^{t-1} \right) = \rho \left(M^\top M \right)^{t-1},$$

where $\| \cdot \|_2$ is the induced 2-norm.

Proof. For a two block Gaussian it holds $\mathbb{E}[\mathbf{x}_{(i)} | \mathbf{x}_{(j)}] = A_{ij} \mathbf{x}_{(j)} + \mathbf{a}_{(i)}$ for $i \neq j \in \{1, 2\}$. So

$$B^{(F)} = \left(\begin{array}{c|c} 0 & A_{12} \\ \hline 0 & A_{21} A_{12} \end{array} \right), \quad B^{(FB)} = \left(\begin{array}{c|c} 0 & A_{12} A_{21} A_{12} \\ \hline 0 & A_{21} A_{12} \end{array} \right). \quad (56)$$

Note that from the above $\rho(B^{(F)}) = \rho(A_{21} A_{12}) = \rho(B^{(FB)})$. One can rewrite (56) as $B^{(F)} = A_2 A_1$ and $B^{(FB)} = A_1 A_2 A_1$ for

$$A_1 = \left(\begin{array}{c|c} 1 & 0 \\ \hline A_{21} & 0 \end{array} \right), \quad A_2 = \left(\begin{array}{c|c} 0 & A_{12} \\ \hline 0 & 1 \end{array} \right). \quad (57)$$

Simple algebra shows that $A_1^2 = A_1, A_2^2 = A_2$ and $(B^{(F)})^t = A_2 (B^{(FB)})^{t-1}$. Furthermore:

$$(N^{(F)})^t = L^{-1} (B^{(F)})^t L = L^{-1} A_2 L L^{-1} (B^{(FB)})^{t-1} L = \tilde{A}_2 (N^{(FB)})^{t-1}, \quad (58)$$

where we defined $\tilde{A}_2 := L^{-1}A_2L$. By symmetry of $N^{(FB)}$ and submultiplicativity of the matrix norm, it follows:

$$\|(N^{(F)})^t\|_2 = \|\tilde{A}_2(N^{(FB)})^{t-1}\|_2 \leq \|\tilde{A}_2\|_2 \rho(N^{(FB)})^{t-1}.$$

If furthermore Q has the form in (55), then one has $A_{12} = M, A_{21} = -M^\top$. Let L^{-1} be such that

$$L^{-1} = \left(\begin{array}{c|c} A & 0 \\ \hline B & C \end{array} \right), \quad (59)$$

It follows

$$\tilde{A}_2 = L^{-1}A_2L = \left(\begin{array}{c|c} 1 & 0 \\ \hline (B - CM^\top)A^{-1} & 0 \end{array} \right),$$

and from (54) it is easy to see that $B = C^{-\top}M = CM$ and so $\|\tilde{A}_2\|_2 = 1$. Plugging the result in (58) gives

$$\|(N^{(F)})^t\|_2 \leq \rho\left(\left(N^{(FB)}\right)^{t-1}\right) = \rho\left(M^\top M\right)^{t-1}.$$

□

Proof of Theorem 2. The result follows from an adaptation of Lemma 7 and Lemma 8 to the case of $K = 2$ blocks, combined with Lemma 10 and Lemma 11 above. Specifically by Lemma 10 and Lemma 11 we have

$$\frac{\|(N^{(F)})^t\|^2}{1 - \lambda_{\min}(N^{(F)}(N^{(F)})^\top)} = \rho(N^{(F)})^{2(t-1)}.$$

And then the sufficient condition in (37) becomes

$$\|L^{-1}(\mathbf{X}^0 - \mathbf{Y}^0)\|^2 \rho(N^{(F)})^{2(t-1)} < 8(\operatorname{erf}^{-1}(\varepsilon))^2.$$

Since then $\rho(N^{(BF)}) = \rho(B^{(FB)}) = \rho(B^{(F)})$, it leads to

$$t > \frac{\ln(\|L^{-1}(\mathbf{X}^0 - \mathbf{Y}^0)\|) - \ln(2\sqrt{2}\operatorname{erf}^{-1}(\varepsilon))}{-\ln(\rho(B^{(F)}))}.$$

Hence one can rewrite the formula for f_1 of Lemma 7 as

$$f_1(r, \varepsilon, B) = 1 + \left\lceil \frac{\ln(r) - \ln(\operatorname{erf}^{-1}(\varepsilon)2\sqrt{2})}{-\ln(\rho(B^{(F)}))} \right\rceil.$$

The final formula is then obtained by plugging the above in the proof of Lemma 8 for f_2 . □

D.3 Proof of Theorem 3

Proof of Theorem 3. With the same reasoning as in Theorem 1, one can show that

$$T \leq 1 + \tilde{f}_1(\|L^{-1}(\mathbf{X}^0 - \mathbf{Y}^0)\|, \varepsilon, B, \delta) + (1 - \varepsilon)^{-1} \tilde{f}_2(\varepsilon, B, \delta),$$

where

$$\tilde{f}_1(r, \varepsilon, B, \delta) = \max \left(n_\delta^*, \left\lceil \frac{\ln(r) - \frac{1}{2} \ln(1 - \rho(NN^\top)) - \ln(\operatorname{erf}^{-1}(\varepsilon)2\sqrt{2})}{1 - \rho(B)} (1 + \delta) \right\rceil \right),$$

and

$$\tilde{f}_2(\varepsilon, B, \delta) = \max \left(n_\delta^*, \left\lceil \frac{\ln(12 + 8\sqrt{2/\pi})\operatorname{erf}^{-1}(\varepsilon)/\sqrt{\pi} + \sqrt{2}(\sqrt{\pi}e)^{-1}}{1 - \rho(B)} (1 + \delta) \right\rceil \right).$$

Then combining the results with the same reasoning as in the proof of Theorem 1 gives the result.

The form of \tilde{f}_1 comes from a generalization of f_1 in Lemma 7. Given (33), a sufficient condition for $\mathcal{D}^t < \varepsilon$ is

$$\|\mathbf{d}^t\|^2 < 8(1 - \lambda_{\min}(NN^\top))(\operatorname{erf}^{-1}(\varepsilon))^2,$$

where as before $N = L^{-1}BL$ (no longer symmetric) and $\mathbf{d}^t = L^{-1}B(\mathbf{X}^t - \mathbf{Y}^t)$. By properties of matrix norm one has

$$\|\mathbf{d}^t\|^2 = \|N^{t+1}L^{-1}(\mathbf{X}^0 - \mathbf{Y}^0)\|^2 \leq \|N^{t+1}\|_2^2 \|L^{-1}(\mathbf{X}^0 - \mathbf{Y}^0)\|^2.$$

The definition of n_δ^* implies that for all $t \geq n_\delta^*$:

$$\|N^t\|_2 \leq \left(1 - \frac{1 - \rho(N)}{1 + \delta}\right)^t = \left(1 - \frac{1 - \rho(B)}{1 + \delta}\right)^t \leq e^{-t\frac{1 - \rho(B)}{1 + \delta}}.$$

Hence if t is bigger than n_δ^* we have

$$\|\mathbf{d}^t\|^2 \leq e^{-(t+1)\frac{1 - \rho(B)}{1 + \delta}} \|L^{-1}(\mathbf{X}^0 - \mathbf{Y}^0)\|^2.$$

Imposing the former to be smaller than $8(1 - \lambda_{\min}(NN^\top))(\operatorname{erf}^{-1}(\varepsilon))^2$ and solving for $t + 1$ leads to the result.

As for \tilde{f}_2 , the result follows from substituting f_1 with \tilde{f}_1 in the proof of Lemma 8. \square

D.4 Proof of the claim in Remark 3

Proof of the claim in Remark 3. Consider a general d -dimensional Gaussian $\pi = N(\boldsymbol{\mu}, Q^{-1})$ divided in K blocks of dimensions I_1, \dots, I_K , for $d = \sum_k I_k$. Lemma 3 of Section 6 shows the equivalence between $\bar{P}_{W_2}[P]$ and \bar{P}^{c*} of (14). As for the maximal coupling, note that the leading term in the computational cost of Algorithm 6 is the cost of the Cholesky decomposition of Q necessary for computing \mathbf{z} , known to be $O(d^3)$. It follows that implementing naively $\bar{P}_{\max}[P]$ has a cost of $O((\sum_k I_k)^3)$, while implementing \bar{P}^{c*} of $O(\max(I_1^3, \dots, I_K^3))$ (for fixed K), since composition of K successive maximal reflection couplings. We show it is possible to implement $\bar{P}_{\max}[P]$ at the same cost. For π above it holds

$$\pi(\mathbf{x}_{(k)}|\mathbf{x}_{(-k)}) = N \left(\sum_{j \neq k} A_{(k,j)} \mathbf{x}_{(j)} + \mathbf{a}_i, Q_{(k,k)}^{-1} \right), \quad (60)$$

where $A = 1_d - \text{diag}(Q_{(1,1)}^{-1}, \dots, Q_{(K,K)}^{-1})Q$ and $\mathbf{a}_i = Q_{(i,i)}^{-1} \sum_{j=1}^s Q_{(i,j)} \boldsymbol{\mu}_{(j)}$. In the following we consider the case of $K = 3$ blocks and forward kernel, although the procedure can be extended straightforwardly to other specifications. A sweep of the Gibbs kernel P of (5) can be written as

$$\begin{aligned}
\mathbf{X}_{(1)}^{t+1} &= A_{(1,2)} \mathbf{X}_{(2)}^t + A_{(1,3)} \mathbf{X}_{(3)}^t + \mathbf{a}_1 + Q_{(1,1)}^{-\frac{1}{2}} \mathbf{Z}_1 \\
\mathbf{X}_{(2)}^{t+1} &= A_{(2,1)} \mathbf{X}_{(1)}^{t+1} + A_{(2,3)} \mathbf{X}_{(3)}^t + \mathbf{a}_2 + Q_{(2,2)}^{-\frac{1}{2}} \mathbf{Z}_2 \\
&= A_{(2,1)} A_{(1,2)} \mathbf{X}_{(2)}^t + (A_{(2,1)} A_{(1,3)} + A_{(2,3)}) \mathbf{X}_{(3)}^t + A_{(2,1)} Q_{(1,1)}^{-\frac{1}{2}} \mathbf{Z}_1 + Q_{(2,2)}^{-\frac{1}{2}} \mathbf{Z}_2 + \mathbf{c}_2 \\
\mathbf{X}_{(3)}^{t+1} &= A_{(3,1)} \mathbf{X}_{(1)}^{t+1} + A_{(3,2)} \mathbf{X}_{(2)}^{t+1} + \mathbf{a}_3 + Q_{(3,3)}^{-\frac{1}{2}} \mathbf{Z}_3 \\
&= (A_{(3,1)} A_{(1,2)} + A_{(3,2)} A_{(2,1)} A_{(1,2)}) \mathbf{X}_{(2)}^t + (A_{(3,1)} A_{(1,3)} + A_{(3,2)} A_{(2,1)} A_{(1,3)} + A_{(3,2)} A_{(2,3)}) \mathbf{X}_{(3)}^t + \\
&\quad + (A_{(3,1)} + A_{(3,2)} A_{(2,1)}) Q_{(1,1)}^{-\frac{1}{2}} \mathbf{Z}_1 + A_{(3,2)} Q_{(2,2)}^{-\frac{1}{2}} \mathbf{Z}_2 + Q_{(3,3)}^{-\frac{1}{2}} \mathbf{Z}_3 + \mathbf{c}_3,
\end{aligned} \tag{61}$$

where $\mathbf{Z}_1, \mathbf{Z}_2, \mathbf{Z}_3$ are Gaussian of dimensions I_1, I_2, I_3 respectively and $\mathbf{c}_2, \mathbf{c}_3$ vectors depending solely on $A, \boldsymbol{\mu}$ and Σ . That is

$$\begin{pmatrix} \mathbf{X}_{(1)}^{t+1} \\ \mathbf{X}_{(2)}^{t+1} \\ \mathbf{X}_{(3)}^{t+1} \end{pmatrix} = B \begin{pmatrix} \mathbf{X}_{(1)}^t \\ \mathbf{X}_{(2)}^t \\ \mathbf{X}_{(3)}^t \end{pmatrix} + \begin{pmatrix} Q_{(1,1)}^{-\frac{1}{2}} & 0 & 0 \\ A_{(2,1)} Q_{(1,1)}^{-\frac{1}{2}} & Q_{(2,2)}^{-\frac{1}{2}} & 0 \\ (A_{(3,1)} + A_{(3,2)} A_{(2,1)}) Q_{(1,1)}^{-\frac{1}{2}} & A_{(3,2)} Q_{(2,2)}^{-\frac{1}{2}} & Q_{(3,3)}^{-\frac{1}{2}} \end{pmatrix} \begin{pmatrix} \mathbf{Z}_1 \\ \mathbf{Z}_2 \\ \mathbf{Z}_3 \end{pmatrix} + \begin{pmatrix} \mathbf{a}_1 \\ \mathbf{c}_2 \\ \mathbf{c}_3 \end{pmatrix}, \tag{62}$$

for B the same of Lemma 1. Since by Lemma 1 we have

$$\begin{pmatrix} \mathbf{X}_{(1)}^{t+1} \\ \mathbf{X}_{(2)}^{t+1} \\ \mathbf{X}_{(3)}^{t+1} \end{pmatrix} = B \mathbf{X}^t + (\Sigma - B \Sigma B^\top)^{\frac{1}{2}} \mathbf{Z} + \mathbf{b}, \tag{63}$$

then equating (62) and (63), it must hold

$$\begin{pmatrix} Q_{(1,1)}^{-\frac{1}{2}} & 0 & 0 \\ A_{(2,1)} Q_{(1,1)}^{-\frac{1}{2}} & Q_{(2,2)}^{-\frac{1}{2}} & 0 \\ (A_{(3,1)} + A_{(3,2)} A_{(2,1)}) Q_{(1,1)}^{-\frac{1}{2}} & A_{(3,2)} Q_{(2,2)}^{-\frac{1}{2}} & Q_{(3,3)}^{-\frac{1}{2}} \end{pmatrix} = (\Sigma - B \Sigma B^\top)^{\frac{1}{2}}.$$

Implementing Algorithm 6 for iteration of teh chains $(\mathbf{X}^t, \mathbf{Y}^t)_{t \geq 1}$, one has $\mathbf{z} := (\Sigma - B \Sigma B^\top)^{-\frac{1}{2}} B (\mathbf{X}^t - \mathbf{Y}^t)$, hence computing \mathbf{z} is actually equivalent to solving the triangular system

$$(\Sigma - B \Sigma B^\top)^{\frac{1}{2}} \mathbf{z} = B (\mathbf{X}^t - \mathbf{Y}^t).$$

Starting from the first coordinate, it can be proved the solution is

$$\mathbf{z}_{(1)} = Q_{(1,1)}^{\frac{1}{2}} \left(A_{(1,2)} (\mathbf{X}_{(2)}^t - \mathbf{Y}_{(2)}^t) + A_{(1,3)} (\mathbf{X}_{(3)}^t - \mathbf{Y}_{(3)}^t) \right).$$

Then

$$\begin{aligned}\mathbf{z}_{(2)} &= Q_{(2,2)}^{\frac{1}{2}} \left(A_{(2,1)} A_{(1,2)} (\mathbf{X}_{(2)}^t - \mathbf{Y}_{(2)}^t) + (A_{(2,1)} A_{(1,3)} + A_{(2,3)}) (\mathbf{X}_{(3)}^t - \mathbf{Y}_{(3)}^t) - A_{(2,1)} Q_{(1,1)}^{-\frac{1}{2}} \mathbf{z}_1 \right) \\ &= Q_{(2,2)}^{\frac{1}{2}} A_{(2,3)} (\mathbf{X}_{(3)}^t - \mathbf{Y}_{(3)}^t),\end{aligned}$$

and lastly

$$\mathbf{z}_{(3)} = 0.$$

From the above it follows that the computational cost of solving for $(\mathbf{z}_1, \mathbf{z}_2, \mathbf{z}_3)$ is exactly $O(\max(I_1^3, I_2^3, I_3^3))$. \square

D.5 Proof of Lemma 3

Proof of Lemma 3. We first show that the distribution induced by \bar{P}^{c*} of (14) is the same as the one induced by $\bar{P}_{W_2}[P]$ of Lemma 6. We then extend the result for the composition of n kernels.

Given any updating order (k_1, \dots, k_K) , let σ be the permutation of $(1, \dots, K)$, such that $(k_1, \dots, k_K) = (\sigma(1), \dots, \sigma(K))$. Define $A = 1_d - \text{diag}(Q_{(1,1)}^{-1}, \dots, Q_{(K,K)}^{-1}) Q$, A^* the matrix whose blocks are $A_{(i,j)}^* = A_{(k_i, k_j)}$ and also $B^* = (I - L^*)^{-1} U^*$, for U^* and L^* upper and lower decomposition of A^* , i.e. $U^* + L^* = A^*$. Lastly define the matrix $B^{(\sigma)}$ as $B_{(k_i, k_j)}^{(\sigma)} = B_{(i, j)}^*$. From Lemma 6 and Lemma 1 of Section 2.1, the W_2 -optimal coupling of P is

$$\bar{P}_{W_2}[P]((\mathbf{x}, \mathbf{y}), \cdot) = N \left(\begin{pmatrix} B^{(\sigma)} \mathbf{x} + \mathbf{b}^{(\sigma)} \\ B^{(\sigma)} \mathbf{y} + \mathbf{b}^{(\sigma)} \end{pmatrix}, \begin{pmatrix} 1 & 1 \\ 1 & 1 \end{pmatrix} \otimes (\Sigma - B^{(\sigma)} \Sigma (B^{(\sigma)})^\top) \right), \quad (64)$$

where $\mathbf{b}^{(\sigma)} = (I - B^{(\sigma)}) \boldsymbol{\mu}$. It follows from Lemma 6 and (60) that $\bar{P}_{W_2}[P_k]$ is

$$\bar{P}_{W_2}[P_k]((\mathbf{x}, \mathbf{y}), (d\mathbf{x}, d\mathbf{y})) = \bar{\nu}[\nu](d\mathbf{x}_{(k)}, d\mathbf{y}_{(k)}) \delta_{(\mathbf{x}_{(-k)}, \mathbf{y}_{(-k)})}(d\mathbf{x}_{(-k)}, \mathbf{y}_{(-k)}), \quad (65)$$

with

$$\bar{\nu}[\nu](d\mathbf{x}_{(k)}, d\mathbf{y}_{(k)}) = N \left(\begin{pmatrix} \boldsymbol{\mu}_{(k)} + A_{(k,:)}(\mathbf{x} - \boldsymbol{\mu}) \\ \boldsymbol{\mu}_{(k)} + A_{(k,:)}(\mathbf{y} - \boldsymbol{\mu}) \end{pmatrix}, \begin{pmatrix} 1 & 1 \\ 1 & 1 \end{pmatrix} \otimes Q_{(k,k)}^{-1} \right).$$

Given that $\bar{P}_{W_2}[P_k] \in \Gamma[P_k]$ for all $k = 1, \dots, K$, it directly follows from the definition of couplings that $\mathbb{E}[\bar{P}^{c*}] = \mathbb{E}[\bar{P}_{W_2}[P]]$, and also the diagonal elements of the variance covariance matrix of \bar{P}^{c*} and $\bar{P}_{W_2}[P]$ must be equal. As for the covariances, if $(d\mathbf{x}, d\mathbf{y}) \sim \bar{P}^{c*}((\mathbf{x}, \mathbf{y}), \cdot)$, for $s = 1, \dots, K$ we have

$$\begin{aligned}d\mathbf{y}_{(s)} - \mathbb{E}[d\mathbf{y}_{(s)}] &= d\mathbf{y}_{(s)} - \boldsymbol{\mu}_{(s)} - \sum_{l=1}^{k_s-1} A_{(s,l)}^* (d\mathbf{y}_{(k_l)} - \boldsymbol{\mu}_{(k_l)}) - \sum_{l=k_s+1}^K A_{(s,l)}^* (\mathbf{y}_{(k_l)} - \boldsymbol{\mu}_{(k_l)}) \\ &= F_s Z_s \\ &= d\mathbf{x}_{(s)} - \boldsymbol{\mu}_{(s)} - \sum_{l=1}^{k_s-1} A_{(s,l)}^* (d\mathbf{x}_{(k_l)} - \boldsymbol{\mu}_{(k_l)}) - \sum_{l=k_s+1}^K A_{(s,l)}^* (\mathbf{x}_{(k_l)} - \boldsymbol{\mu}_{(k_l)}) \\ &= d\mathbf{x}_{(r)} - \mathbb{E}[d\mathbf{x}_{(s)}],\end{aligned}$$

where F_s such that $F_s F_s^\top = (Q^{-1})_{(s,s)}$, $Z_s \sim N(\mathbf{0}_{I_s}, \mathbf{1}_{I_s})$. For every $1 \leq r < s \leq K$, it follows

$$\begin{aligned} \text{cov} \left(d\mathbf{x}_{(r)}, d\mathbf{y}_{(s)} \right) &= \mathbb{E} \left[(d\mathbf{x}_{(r)} - \mathbb{E}[d\mathbf{x}_{(r)}]) (d\mathbf{y}_{(s)} - \mathbb{E}[d\mathbf{y}_{(s)}])^\top \right] \\ &= \mathbb{E} \left[(d\mathbf{x}_{(r)} - \mathbb{E}[d\mathbf{x}_{(r)}]) (d\mathbf{x}_{(s)} - \mathbb{E}[d\mathbf{x}_{(s)}])^\top \right] \\ &= \text{cov} \left(d\mathbf{x}_{(r)}, d\mathbf{x}_{(s)} \right) \\ &= \left(\Sigma - B^{(\sigma)} \Sigma (B^{(\sigma)})^\top \right)_{(r,s)}, \end{aligned}$$

hence the result for $n = 1$.

We now prove the result for $n \geq 2$. Given $\bar{P}^{c*} = \bar{P}_{W_2}[P]$ as proved above and leveraging the equivalent formulation in (7) along with properties of Gaussian distribution, it follows that iterating n times $P(\mathbf{x}, \cdot)$ is the same as

$$P^n(\mathbf{x}, \cdot) \stackrel{d}{=} N \left((B^{(\sigma)})^n \mathbf{x} + \left(\sum_{j=0}^{n-1} (B^{(\sigma)})^j \right) \mathbf{b}^{(\sigma)}, \left(\sum_{j=0}^{n-1} (B^{(\sigma)})^j \right) \left(\Sigma - (B^{(\sigma)}) \Sigma (B^{(\sigma)})^\top \right) \left(\sum_{j=0}^{n-1} (B^{(\sigma)})^j \right)^\top \right).$$

Suppose that $(d\mathbf{x}', d\mathbf{y}') \sim (\bar{P}_{W_2}[P])^n((\mathbf{x}, \mathbf{y}), \cdot)$, then

$$\mathbb{E}[\|\mathbf{x}' - \mathbf{y}'\|^2] = \|(B^{(\sigma)})^n \mathbf{x} - (B^{(\sigma)})^n \mathbf{y}\|^2 = W_2(P^n(\mathbf{x}, \cdot), P^n(\mathbf{y}, \cdot)).$$

□

D.6 Proof of Lemma 5

Proof of Lemma 5. By (32), and the definition of \bar{c}_d , it holds

$$\|p - q\|_{TV} = \text{erf} \left(\bar{c}_d d^{-\alpha + \frac{1}{2}} \right). \quad (66)$$

If $\alpha > \frac{1}{2}$, as $d \rightarrow +\infty$, Taylor expanding the *erf* function around 0 gives

$$\Pr_{\max}(p, q) = 1 - \|p - q\|_{TV} \asymp 1 - \frac{2\bar{c}_d}{\sqrt{\pi}} d^{-\alpha + \frac{1}{2}}. \quad (67)$$

If instead $0 < \alpha < \frac{1}{2}$, the argument of the *erf* function goes to $+\infty$. We exploit Gaussian tail bounds to characterize the behaviour. Recall indeed that

$$\text{erf}(x) = 2\Phi(\sqrt{2}x) - 1,$$

$$\Pr_{\max}(p, q) = 1 - \text{erf} \left(\bar{c}_d d^{-\alpha + \frac{1}{2}} \right) = 2 \left(1 - \Phi \left(\sqrt{2} d^{-\alpha + \frac{1}{2}} \bar{c}_d \right) \right),$$

where $\Phi(\cdot)$ indicates the standard Gaussian cumulative. Furthermore for x going to infinity, it holds $1 - \Phi(x) \asymp \frac{\phi(x)}{x}$, where ϕ denotes the density function of the standard Gaussian, it follows

$$\Pr_{\max}(p, q) \asymp \frac{d^{\alpha - \frac{1}{2}}}{\sqrt{\pi} \bar{c}_d} e^{-\frac{\bar{c}_d^2}{\sqrt{2}} d^{-2\alpha + 1}}.$$

On the other hand, considering the product of independent maximal couplings, the argument

of each erf function goes to 0 as $d \rightarrow +\infty$ and hence we exploit the same expansion as in (67), getting

$$\begin{aligned} \prod_{i=1}^d \Pr_{max}(p_i, q_i) &= \prod_{i=1}^d \left(1 - erf \left(d^{-\alpha} \sqrt{\frac{c_i^2}{8}} \right) \right) \\ &= \prod_{i=1}^d \left(1 - \frac{|c_i|}{\sqrt{2\pi}} d^{-\alpha} + o(d^{-\alpha}) \right) \asymp e^{-d^{1-\alpha} \tilde{c}_d}, \end{aligned}$$

where $\tilde{c}_d = \frac{\sum_{i=1}^d |c_i|}{d\sqrt{2\pi}}$. □